Effects of A Solution Anneal Quench Delay on the Heat Treatment Response of Aluminum 2219-T6

Daniel J Filomeo

Senior Project Report

June 4th, 2010

Advisor

Dr. Blair London

Material Engineering Department

California Polytechnic State University, San Luis Obispo

Approval Page

Project Title: Effects of A Solution Anneal Quench Delay on the Heat Treatment Response For Aluminum 2219-T6

Author: Daniel Filomeo

Date Submitted: June 4, 2010

CAL POLY STATE UNIVERSITY
Materials Engineering Department

Since this project is a result of a class assignment, it has been graded and accepted as fulfillment of the course requirements. Acceptance does not imply technical accuracy or reliability. Any use of information in this report is done at the risk of the user. These risks may include catastrophic failure of the device or infringement of patent or copyright laws. The students and staff of Cal Poly State University, San Luis Obispo cannot be held liable for any misuse of the project.

Prof.
Faculty Advisor _____ Signature

Prof. Trevor Harding
Department Chair _____ Signature

Abstract

The ageing response for aluminum 2219-T6 was investigated to determine the effects a quench delay (QD) could have on tensile properties. Before testing commenced, furnace surveys were conducted to ensure they could meet the required temperature stability of ± 10˚F (±6˚C). MIL-H-6088 specified a maximum quench delay of 15 seconds for parts thicker than 2.29 mm (0.090 in). An investigation was conducted on how different quench delay times changed the ageing response of T6 heat treated for Al 2219. Heat treatments were performed according to the ASM Handbook. Preliminary tests were performed on 1-1.5 in. cube blocks of Al 2219 and the ageing response was tracked using hardness. Later tests were conducted using flat tensile coupons. To relate the quench delay to the material temperature, cooling curves were made for the cubes and tensile samples. For the preliminary tests, quench delays of 15, 25, and 35 seconds were used which all yielded average hardness values ranging from 72-76 HRB and standard deviations ranging from 2-6 HRB. Using results from preliminary tests, the tensile samples had quench delays of 5, 10, 15, 20, and 25 seconds. There was a difference in yield and tensile strength for the samples with a 5 second QD when compared to samples with a 20 second and 25 second QD. To pass quality insurance the parts needed to have a yield strength above 276 MPa, tensile strength above 400 MPa, and elongation of 6% at 4 times the width of the samples. The yield strengths ranged from 271-315 MPa along with tensile strengths of 390-430 MPa. The ductility of the samples ranged from 15 to 18% elongation.

KEYWORDS

Aluminum 2219, Heat Treatment, Solution Anneal, Quench Delay, Precipitation Hardening, Artificial Ageing, Tensile Testing, Hardness Testing

Table of Contents

List of Figures

List of Tables

Introduction

Weber Metals (Paramount, Ca) is an aluminum and titanium forging company that specializes in products for many different industries. Some of the major industries that Weber Metals serves include commercial aerospace, military aerospace, various space programs, and electronic/ semiconductor industries. Weber is currently experiencing some challenges with the production consistency of aluminum alloy 2219. There is scatter in the tensile properties of the forged and heat treated Al 2219-T6 components. Weber has been looking into the different possibilities for why the tensile properties, specifically yield strength, tensile strength, and % Elongation, are showing scatter.

Aluminum (Al) 2219 is commonly used in applications such as the construction of liquid cryogenic rocket fuel tanks because of useful properties such as good weldability, high strength to weight ratio and superior cryogenic properties.[1] Other applications include welded space booster oxidizer/fuel tanks, supersonic aircraft skins, and welded structural components.[2] Because Al 2219 is commonly used in structural applications where strength is a necessity, it would be reassuring to know that parts that come from the same batch or different batches have the same properties. It would be costly, for any manufacturer, to quality check every part that is produced on its production line. Typically, a few parts in a batch are checked for quality assurance and if all properties pass inspection, the whole batch passes.

The goal of this project is to quantify the effects of the quench delays, during the age hardening heat treatment, on the tensile properties of the material. Currently there is an industry standard of 15 second maximum time delay for the quench as specified by MIL-H-6088. The quench delay is the time that is required to move the part from the furnace to the quench tank following the solution anneal. The delay time is defined as the time between opening the furnace door and

fully submerging the part in the quench media. If the part cannot be fully submerged within 15 seconds then the part should remain above about 400°C.[3] Using cooling curves, the temperature decrease in the solution annealed part can be determined for a 15 second quench delay. Because different sized and shaped parts will cool at different rates due to surface area and volume differences, a set time delay will not have the same effect on all parts. The material temperature is more important to the heat treatment response rather than the time delay. Tensile tests will be used to relate the heat treatment response of Al 2219 for different quench delays. The quench delays will be correlated to the material temperature to determine the minimum temperature for Al 2219 to respond to the precipitation hardening heat treatment effectively. The quench delay will also allow changes in tensile properties to be correlated to the material temperature.

Even though the Al alloy is recommended to have a minimum temperature of 415°C, Al 2219 does not have a single phase solution region because the amount of Cu is beyond 5.65 wt% solubility limit. This means that as soon as the material begins to cool Cu begins to diffuse out of solution. In the Al-Cu system the shallow slope of the solvus line near the 2219 alloy composition line indicates that a slight decrease in temperature can result in a large reduction of Cu in solution (Figure 1).[4]

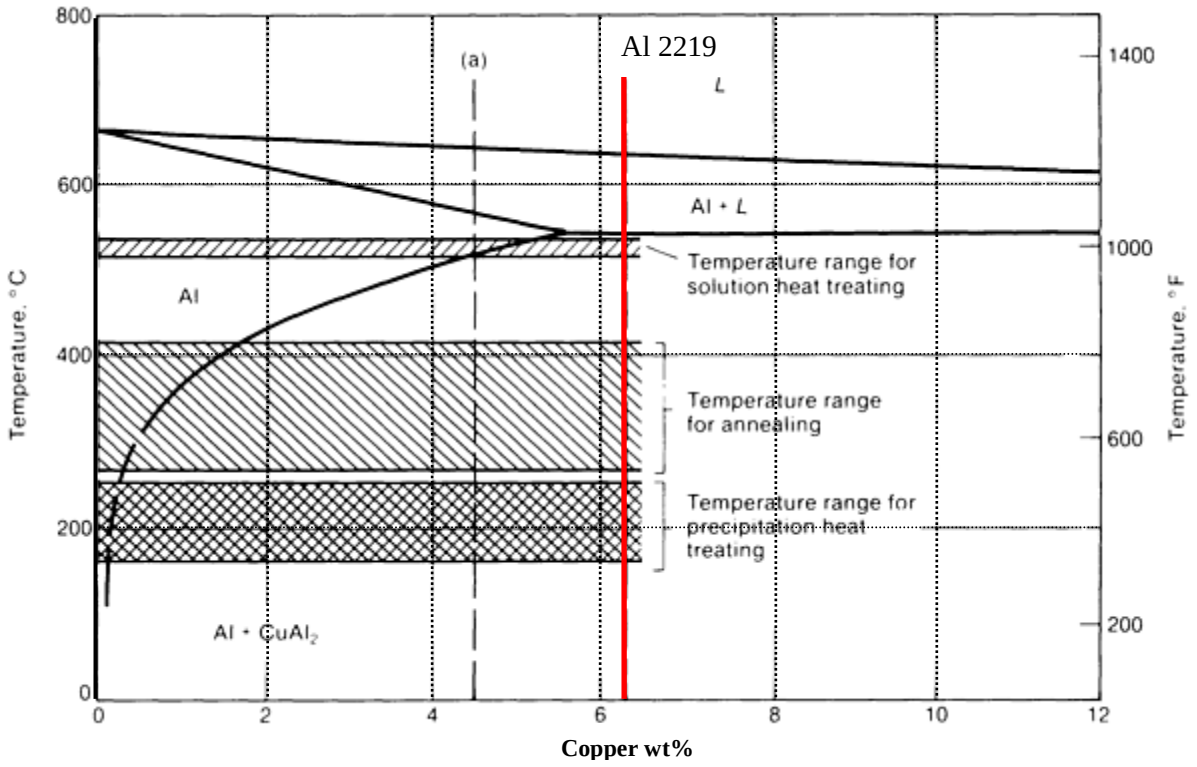

Figure 1: The solvus line of Al-Cu is shallow because the Cu concentration in the single phase solid solution is highly dependent on temperature. The Cu concentration can have a large effect on the material's strength after heat treatment.[5]

The less Cu that is in solution the less Cu is available to precipitate and form $CuAl_2$ (the strengthening precipitate) resulting in a decrease in strength. So the difference of a few degrees for the solution anneal quench can have a large impact on the strength of the Al 2219 when it is heat treated. Table I shows how a small temperature change for Al 2024 effects the tensile and yield strength of the material.

Table I: Solution Anneal Temperature Effect on the Strength of Al 2024- T4[6]

Solution Anneal Temperature		**Tensile strength**		**Yield strength**	
°C	**°F**	**MPa**	**ksi**	**MPa**	**ksi**
488	910	419	60.8	255	37.0
491	915	422	61.2	259	37.5
493	920	433	62.8	269	39.0
496	925	441	63.9	271	39.3

Table I shows the importance of the quench delay because if the parts Weber Metals is producing are cooling at different rates and times, then different parts within the same batch or between batches can have variation in mechanical properties.

Precipitation Hardening of Aluminum

Precipitation hardening, or age hardening, provides one of the most widely used mechanisms for strengthening many alloys. The fundamental understanding and basis for this technique was established in early work at the U. S. Bureau of Standards on an alloy known as Duralumin.[7] Duralumin is a trade name aluminum alloy containing copper and magnesium with small amounts of iron and silicon. This was the first studied precipitation hardened aluminum alloy used in engineering applications.

The following information discusses the general process of precipitation hardening; however, the Al-Cu alloys system is exemplified because Al 2219 is an Al-Cu alloy. The copper atoms are the alloying element of Al 2219 which aid in the formation of the precipitates and will be referred to as the solute. The process for precipitation hardening an alloy involves three steps: solution anneal (SA), quench, and age. However, not all materials are suitable for precipitation hardening. For a material to be suitable for precipitation hardening it must contain alloying elements which have a decreasing solubility with decreasing temperature (Figure 2).[8] Pure metals cannot be hardened by this mechanism. Another requirement is that during the ageing process the precipitate must form on a fine scale to prevent dislocation loops forming between the particles. The final requirement is that the precipitate that forms must provide a barrier for dislocation motion.

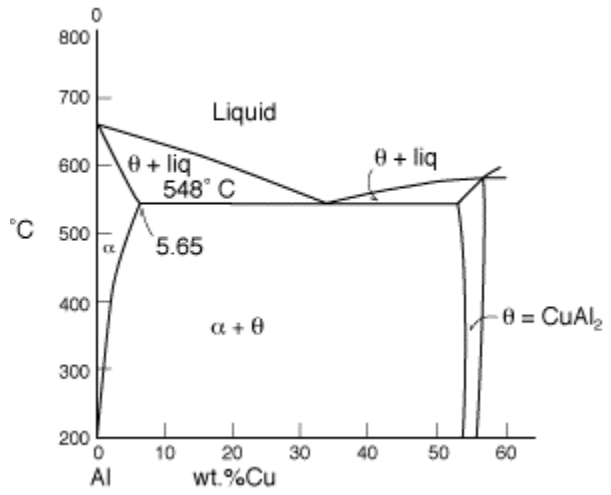

Figure 2: The Al-Cu phase diagram shows the solubility of copper decreases as the temperature decreases (between 5.65 wt.% and 0) which allows Al-Cu alloys to be precipitation hardened. [9]

During the solution anneal the alloy is raised to an elevated temperature which increases the solubility of the solute within the solvent (Figure 3). The solution anneal is generally done in a single phase region so that the maximum amount of solute is dissolved within the solvent. However this is not always necessary since Al-2219 has 5.8-6.8 wt% Cu which is beyond the single phase solubility limit.[10] In this case a single phase region cannot be attained, the goal is to dissolve as much solute as possible without getting too close to the point where the material will begin incipient melting. The SA temperature also must take into account fluctuation in the furnace to avoid overheating which can degrade the tensile strength, fracture toughness, and ductility of the material.[10]

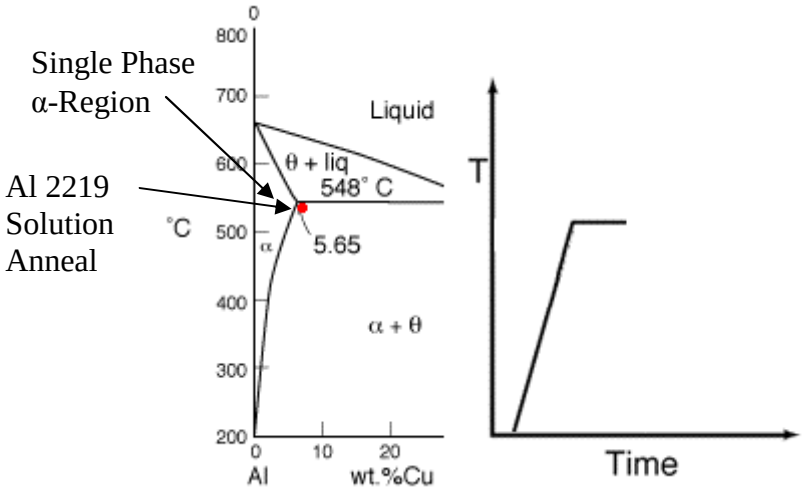

Figure 3: The relationship between the phase diagram and the time-temperature graph for the solution anneal step in precipitation hardening. The alloy is raised to an elevated temperature for a period of time to maximize the solute solubility and evenly dissolve the Cu atoms.[9]

The alloy is held at elevated temperatures for a time period specified by the heat treatment. The time hold at elevated temperature allows a maximum amount of solute to dissolve and homogeneously disperse within the solvent, which is important to ensure uniform properties throughout the material (Figure 4).

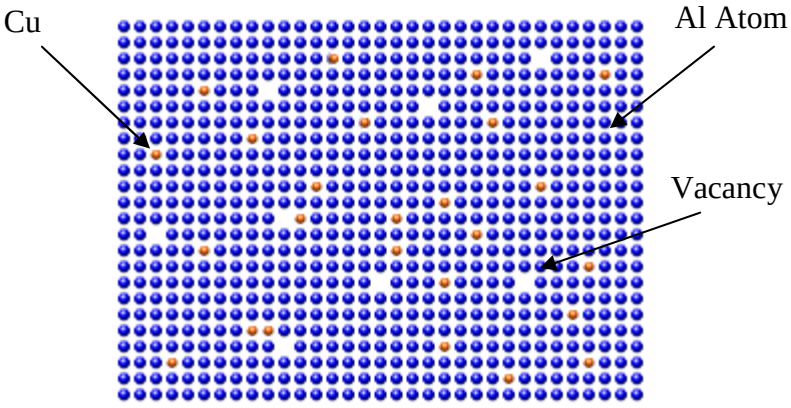

Figure 4: The Cu atoms (orange) are homogenously distributed throughout the α-matrix (blue). Notice at the higher temperatures vacancies are present in the material.[11]

The material is then quenched, trapping the dissolved Cu atoms in a metastable supersaturated solid solution (SSS) (Figure 5). If the alloy is not quenched, the solute will diffuse out of solution as the solubility limit decreases, reducing the effectiveness of the solution anneal. The rapid

quench does not allow adequate time for the Cu atoms to diffuse out of solution so they become trapped or frozen in solution. At the lower temperatures there is a large driving force for the Cu atoms to form a more stable θ phase because, thermodynamically, the solution is beyond its equilibrium saturation level. However, at the low temperatures there is insufficient thermal energy for the Cu to diffuse within the α-matrix.

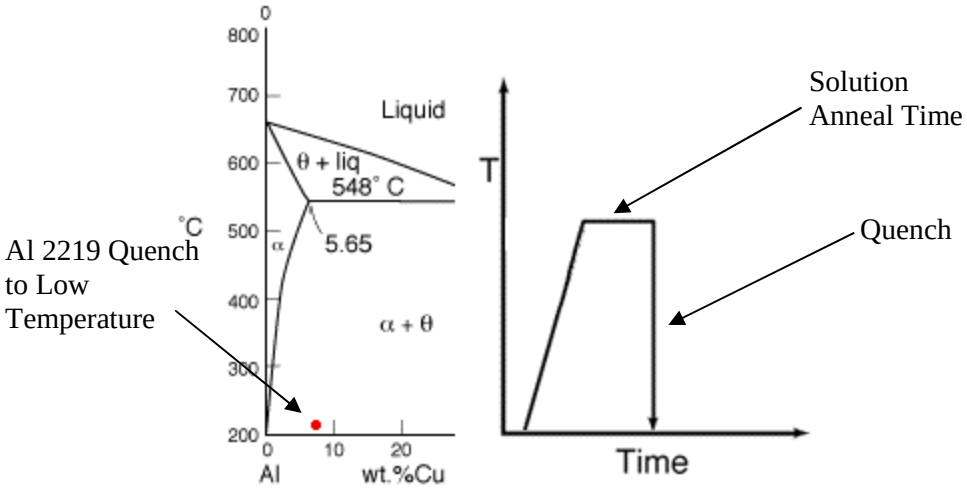

Figure 5: After the solution anneal, the alloy is rapidly quenched to trap the supersaturated Cu atoms in solution. This also traps the vacancies as well, which will later provide nucleation sites for Cu-rich precipitates.[9]

The quench media can vary from various salt baths, oils, or water. The media can range in temperatures from room temperature to that of boiling water.[12] Typically aluminum alloys are not quenched much below room temperature or above 100°C, but other alloys such as steels can have more extreme quench temperatures. Likewise, the quench is not limited to a single step process. Some heat treatments can have multiple quench steps in multiple media to reduce distortion, reduce thermal shock (cracking), provide a specific microstructure, and improve corrosion resistance. The proper combination of media and temperature is dependent upon the desired properties and the alloy system. The steps used in a typical heat treatment process are usually a compromise to provide the best overall combination of properties.[13] For example,

Ausformed steels are quenched to elevated temperatures around 600°C, drawn, and re-quenched at 350°C to provide a unique bainite microstructure.[14]

After the quench, the material can be aged naturally or artificially. A natural age is done at room temperature under natural conditions and the artificial age is performed at elevated temperatures. The elevated temperatures (lower than the solution anneal temperature) artificially speeds up the growth and development of the $CuAl_2$ (θ) precipitates by allowing quicker diffusion (Figure 6).

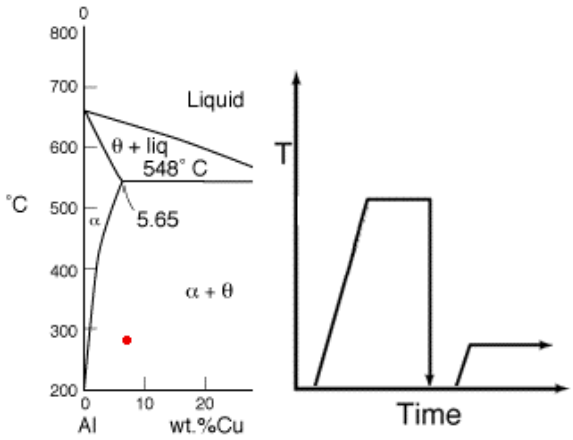

Figure 6: Following the quench, the alloy is raised to an elevated temperature for a period of time to allow the θ precipitates to form and grow. The ageing process is followed by a second quench to stop the growth of the precipitates.[9]

The ageing process is the gradual decomposition of the SSS as the alloying elements or compounds begin to form small precipitates in the solvent. Artificial ageing provides extra thermal energy to the system which allows the solute to diffuse within the solvent and precipitate out of solution. The typical sequence for the decomposition of the Al-Cu SSS is:

$$\alpha_0 \rightarrow \alpha_1 + \text{GPZ} \rightarrow \alpha_2 + \theta'' \rightarrow \alpha_3 + \theta' \rightarrow \alpha_{eq} + \theta \qquad (1)$$

where α is the single phase solution of Al and Cu, GPZ stands for Guinier-Preston (GP) zones, θ″ and θ′ are transitional phases of the intermetalic θ, $CuAl_2$. The subscripts on α refers to the decreasing Cu composition in the α-phase as it precipitates out of solution. The microstructure evolution sequence for the Al-Cu system is shown in Figure 7.

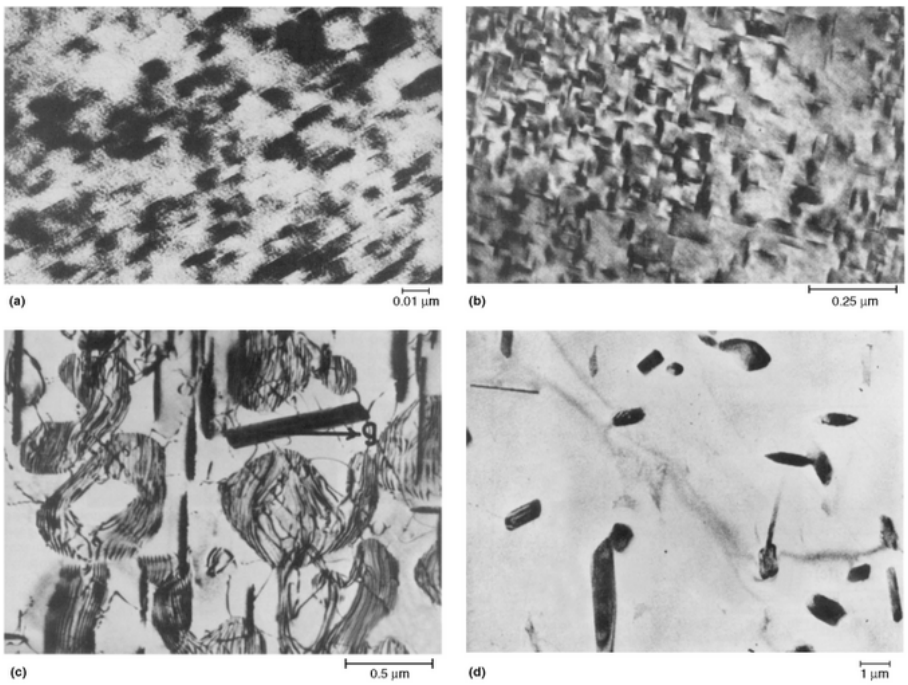

Figure 7: Transmission electron micrographs of precipitation sequence in aluminum-copper alloys. (a) Guinier-Preston zones at 720,000×. (b) θ″ at 63,000×. (c) θ′ at 18,000×. (d) θ at 8000×.[15]

GP zones form as multiple Cu atoms come together on a single plane and begin to create stress fields with in the Al matrix (Figure 8). The θ phase will usually begin to nucleate at the sites of vacancies where Cu atoms can diffuse out. The Al-matrix around the GP zones distorts from the presence of the new phase which leads to coherency strain (misfit strain) in the lattice. The strain is caused by the size differences of the atoms. Because the Cu atom is larger than the Al atom, the Cu atoms form compression stress fields as they squeeze into a small vacancy.

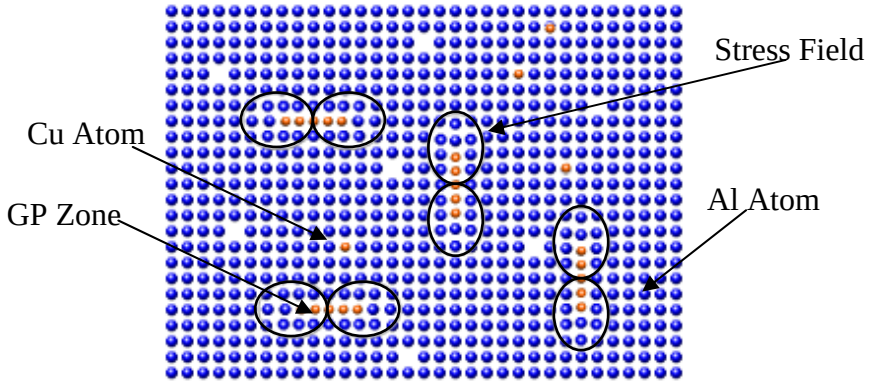

Figure 8: As the Cu atoms coalesce they form regions of coherency strain as the mismatched-atomic-sized particles try to fit into the Al-matrix.[11]

When the solvent and solute atoms are about equal in size (Al-Ag) the GP zones will typically form spherical clusters. When the solvent and solute atoms have a large size difference, such as Al and Cu, the GP zones usually form disks parallel to a low-index plane of the matrix lattice (close-packed slip planes).[16] The GP zones provide nucleation sites for a coherent intermediate phase which form as more Cu atoms diffuse together (Figure 9). As the precipitates become larger the strain increases, which can produce dislocations as a partial means to relieve stress.

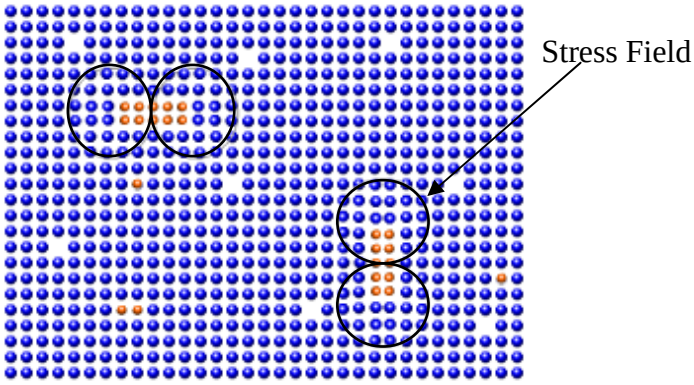

Figure 9: As more Cu atoms come together, the stress fields increase as more Cu atoms try to fit into the Al-lattice.[11]

As the particles become large enough, they form their own equilibrium phase with a crystal structure distinct from the original Al matrix. The structures of the θ′ and θ phases are tetragonal (TET) and body-center tetragonal (BCT), respectively.[17] Because the TET and BCT structures are different from aluminum's face-center cubic (FCC) structure they form semi-coherent boundaries. Larger precipitates are semi-coherent because the new distinct structures do not match the FCC lattice perfectly which decreases the lattice strain. The semi-coherent boundaries still produce coherency strains in the lattice as the mismatching structures attempt to align; however, the formation of a separate crystal structure reduces the coherency strain between the two phases. Because the planes are no longer in one-to-one alignment for the matrix and precipitate, the amount of strain in the α-matrix allowing the planes to line up is decreased. However, the reduced coherency strain is replaced by the surface energy created between the

interphase boundary of the matrix and precipitate (Figure 10). The overall energy level of the system is reduced by the formation of the second phase. For the boundary to form, the surface energy produced must be less than the strain energy reduced.

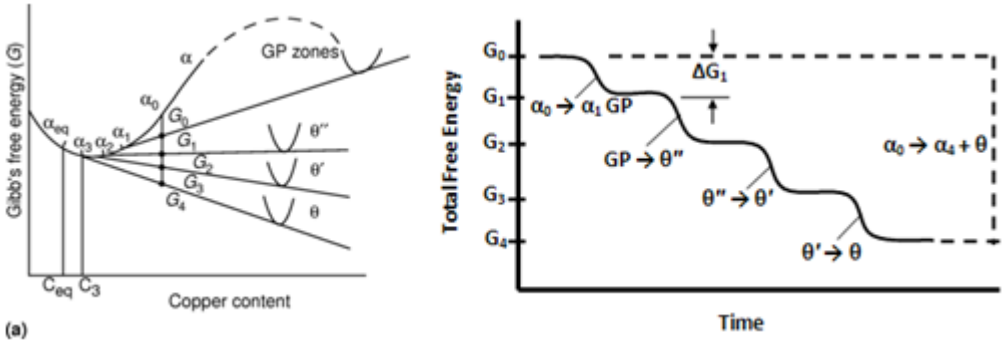

Figure 10: Free-energy plots of precipitation sequence in aluminum-copper alloys shows the decrease in overall energy. (a) Free-energy curve with common-tangent points for phase compositions in the matrix. (b) Step reductions in the free energy as the transformation proceeds. C_{eq} and C_3, copper content of α_{eq} and α_3 phases; ΔG_1, activation energy for $\alpha_0 \rightarrow \alpha_1$ + GP.[18]

As the particles increase in size they reach a point where the precipitate phase becomes completely incoherent (Figure 11). At this stage the coherency strain in the lattice reduces to almost zero and is replaced by the surface energy required to have a distinct boundary. The elimination of the coherency strains also eliminates the stress fields surrounding the precipitates.

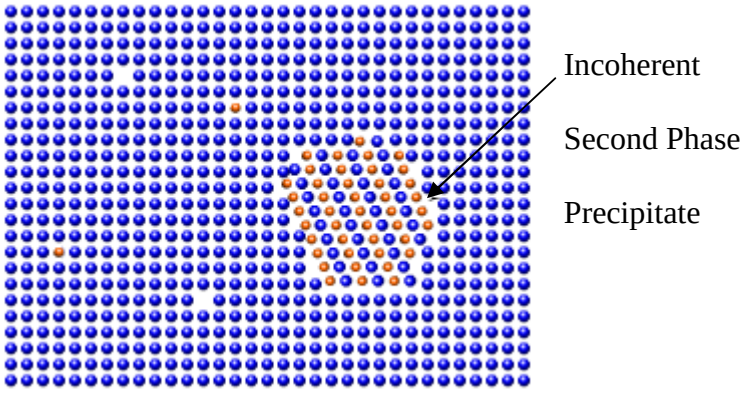

Figure 11: The stress field associated with the coherency strain is eliminated when the particles form a separate incoherent phase within the α-lattice.[11]

Some of the main benefits of the heat treating process besides increasing the strength of th alloy are the effects that the precipitates have on the material's resistance to creep, wear, fatigue, and corrosion.[17]

Dislocation Motion and Interactions with Precipitates

Plastic deformation in metals and alloys occurs from the motion of dislocations in the structure. The easier the dislocations can move, the less stress is required to plastically deform the material. Through the formation of the precipitates, the motion of dislocations is restricted within the material. Each stage of the precipitate's evolution acts to impede the motion of dislocations. The size, shape, spacing, and orientation of the precipitates, which can be controlled by the ageing processes, have a strong influence on the plastic deformation behavior of an alloy. Precipitates can influence the initial yield strength and the hardening behavior by how they interact with dislocations. As mentioned earlier, the precipitates of an Al-Cu alloy align on the close-packed slip planes of the crystal structure on which dislocations glide. Typically sized precipitates have diameters about 1 μm and thicknesses on the order of 0.05 μm. In relation to a typical grain diameter which is on the order of 500 μm, the precipitates are much smaller. Several mechanical models related to these hardening effects have been suggested for Al–Cu alloys containing θ precipitates with a volume fraction of 2–3%.[19] The three common hardening mechanisms that impede dislocation are coherency hardening, chemical hardening, and dispersion strengthening.[11] At high strengths the alloy utilizes a combination of all three mechanisms.

Coherency hardening is caused by the GP zones. They slow the dislocations as they pass through the stress (or strain) fields formed by the coherency strain on the lattice (Figure 12). The GP

zones are areas where a small number of Cu atoms group together coherently with the surrounding matrix.

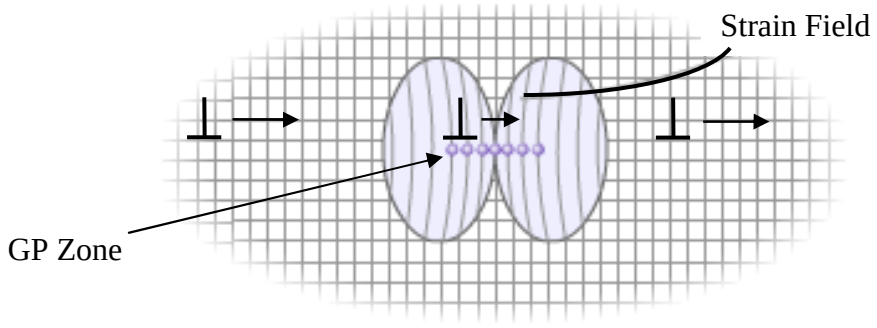

Figure 12: The dislocation slows as it encounters the strain field of the GP zone.[11]

An additional form of strengthening known as chemical hardening (or strengthening) is related to the energy required to increase the area of precipitate/matrix interface as the particle is sheared (Figure 13). To overcome the presence of particles, dislocations will either shear through them or bow around them.[20] The ability of the dislocation to shear the particles depends on particle structure, alignment, and shear modulus. Dislocations travel on paths of least resistance so when the dislocation interacts with a precipitate the dislocation must shear through a material with a different shear modulus, G. If G for the precipitate (G_p) is greater than G of the matrix (G_m) the dislocation would be hindered at the interface of the matrix and precipitates. If G_p is less than G_m the dislocation is trapped at the interface between the precipitate and the matrix and the continued motion past the precipitate becomes hindered. Hindering the motion of the dislocation strengthens the material by slowing or preventing its propagation. Shearing can occur for semi-coherent precipitates depending on the severity of the particle's misalignment with the matrix and shear modulus. Additional strengthening can also be achieved if the particles have low stacking fault energies or exhibit ordered crystal structures.[11]

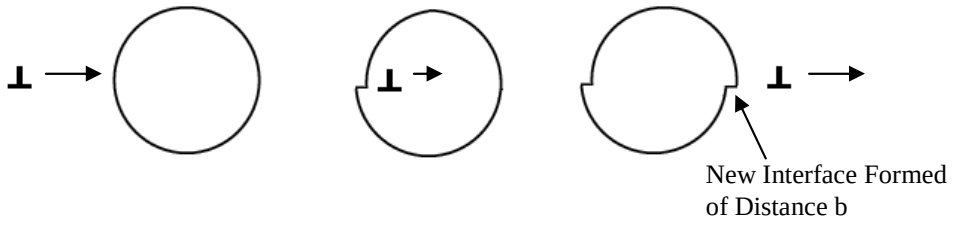

Figure 13: As a dislocation approaches a coherent precipitate the dislocation must shear though a material with a different shear modulus, slowing the movement. The particle is sheared by a distance b (the Burger vector). The diagram assumes the slip plane of the particle lines up with the slip plane of the matrix (coherent interface).[9]

The larger precipitates, that form incoherent phases, block dislocation motion through dispersion hardening. Since the precipitate is not coherent the dislocation cannot readily pass though the particle because the slip planes do not coincide. For a dislocation to pass an incoherent precipitate, it must move around the particles by jumping to a different slip plane, a process called double kinking, or by bowing (Figure 14). Bowing occurs as the dislocation begins to bend around the precipitate. Eventually the bowing segments will join, at which point, dislocation can then proceed while leaving a dislocation loop around the particle.[19] Bowing/ Orowan looping is more likely to happen for larger precipitates because the dispersion is more spread out, providing larger gaps between the particles for the dislocation to move through. Some aluminum alloys can be cold worked prior to the ageing process to improve the heat treatment response. Al 2219 can nucleate a finer dispersion of precipitates leading to higher strengths when cold worked between the quench and age.

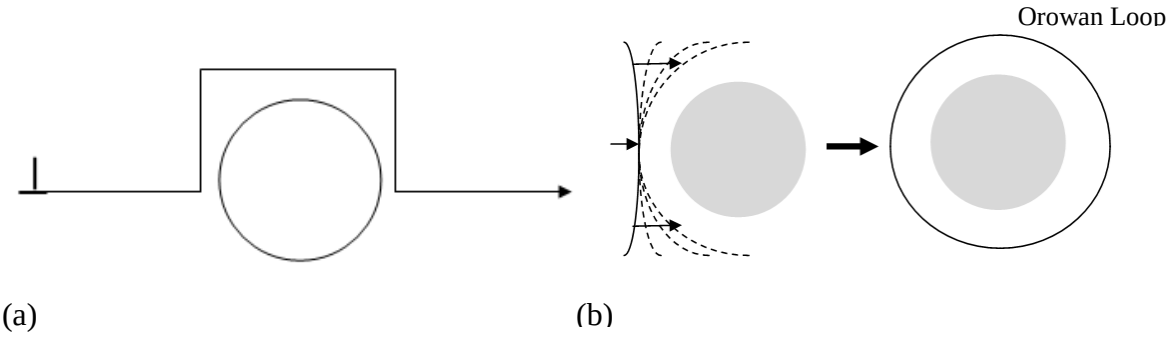

Figure 14: (a) Dislocations move around non-shearable precipitates by double kinking. (b) If precipitates are spaced apart enough, dislocations can move through or around the precipitate by bowing which can form Orowan Loops.

Another way to look at the interaction of precipitates and dislocations is shown in Figure 15. Computer modeling was used to determine the interaction and how the coherency of the precipitates can change the behavior of the dislocation motion. The computer modeling shows how dislocation paths change when they encounter a precipitate. The scenario shown in Figure 15(a) will eventually lead to the formation of an Orowan loop.

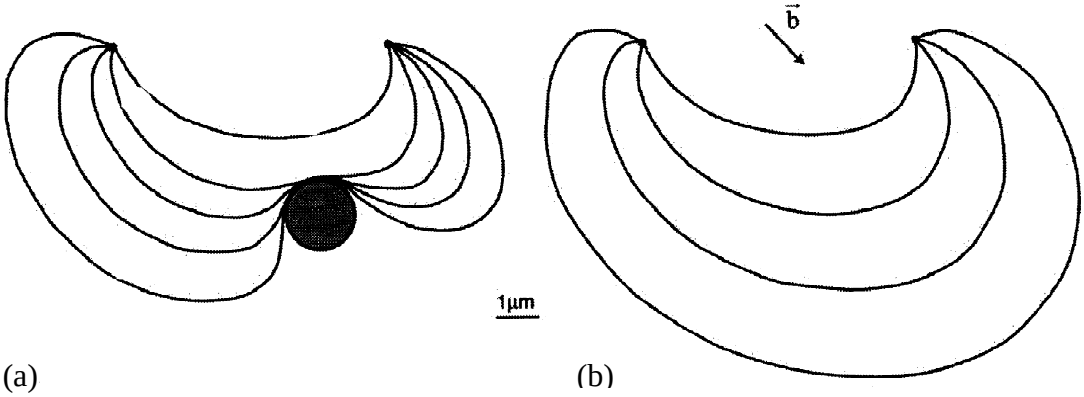

Figure 15: (a) Simulated interaction of a dislocation segment with a perfectly coherent precipitate. The dislocation is pinned between two points; (b) movement of the same segment in the absence of the precipitate. The shear stress acting on the dislocation is 50 MPa.[21]

It is important to understand the impact that the precipitates have on an alloy. Commercially pure aluminum (CP Al) has a yield strength and tensile strength around 25 MPa and 58 MPa, respectively. [22] A major reason for the low strength has to do with Al's FCC crystal structure which allows the material to be easily deformed because it has many slip systems. Besides the many slip systems, CP Al also has few lattice impurities to hinder dislocation motion (no alloying elements or precipitates) which further reduces strength. However, Al 2219, and other alloys, can be precipitation hardened to increase the yield strength and tensile strength. Al 2219 in the T6 condition can have a yield strength and tensile strength around of 260 MPa and 400 MPa respectively. Al 2024, which is similar to 2219 but with about 4 wt% Cu, when annealed has a yield strength of about 75 MPa and in the T6 condition the yield strength increases to about 363 MPa. By comparing Al 2024 and CP Al the effect and magnitude of the precipitates can be

seen, compared to alloying elements alone, on the material properties. Adding alloying elements increases the yield strength from about 25 MPa for CP Al to 75 MPa for Al 2024. The formation of the precipitates however, further increases the yield strength to 363 MPa. While the alloying elements help to strengthen the alloy, the real strength potential is provided by the precipitates.

Broader Impacts

It is part of engineering to understand the importance of a project and how the project is beneficial in an overall sense. Even though aluminum alloys have been around and have had so much research performed on them for various manufacturing purposes, there is still much to be explored. A lot of research done on the production and manufacturing of a material is done by private companies for specific projects which limits the information available for general use. It is not uncommon for companies to use generic manufacturing process that have been used in the past to create successful products. However, a particular processing method may work for one material, but not another. A process that may work for one product may not work for another product even if it is made of the same material. Assuming that a particular process works, it does not mean that it is the best suited or most efficient process for a product. In order to select the best process the company must take into account the details of the product such as size, shape, and what materials are involved. By having an understanding of the material and its processing limitations, a process can be chosen that can maximize production efficiency and yield the desired properties.

Bringing an engineering background to a manufacturing application allows companies to tailor their production process to produce higher quality and more cost effective parts. As the requirements for different products change, the process can be altered to accommodate these variations such as changes in the size, shape, mechanical properties, and material choice of the

part. If a product is not meeting required properties then the process can be altered based on how the material is behaving.

Being able to relate the alloy temperature when it is quenched to mechanical properties can be useful when designing a part or when laying out a manufacturing plant. Using finite element analysis on a design the cooling rates and temperature of a part can be determined for different delay times. Since not all parts cool at the same rate or even all sections of the same part, finite element analysis can help to determine where the low temperature regions are located. If a particular delay time produces areas that fall below some minimum temperature in which it will not respond adequately to the heat treatment, the part can be redesigned or the processing can be changed. When laying out a manufacturing plant the quench tanks should be close enough to the solution anneal furnaces so that the parts can be transferred from the furnace to the forging press or quench tank without cooling below some minimum value. If you know how long a part can be in the air before it reaches this minimum temperature value it can provide an idea of how the manufacturing plant should be laid out.

Experimental Procedures

Before investigating the effects of the quench delay, an assessment of the heat treatment furnaces needed to be conducted. The assessment of the thermal stability and the thermal gradients of the furnace were measured with thermocouples placed throughout the furnace.

Calibrating the Thermocouples

Type K thermocouples were used to measure the heat treatment furnaces. To ensure that the thermocouples are reading the proper temperature they must be calibrated before being used to measure temperatures in a furnace. Three points of known temperature were used to calibrate the

thermocouples: boiling water, ice water, and a point in between the two. The temperature of the water was measured using a mercury thermometer as well to ensure the accuracy of the thermocouples.

Preparing Samples for Furnace Testing

To survey the temperature distribution in the furnace, multiple thermocouples must be placed into the furnace and secured at specific locations. If the thermocouples move in the furnace then the tests would not be meaningful. To secure the thermocouples in place they were placed into one inch blocks of aluminum (Figure 16). The aluminum blocks, while securing the thermocouples, aided in determining not just the furnace temperature but also the material temperature at a given location.

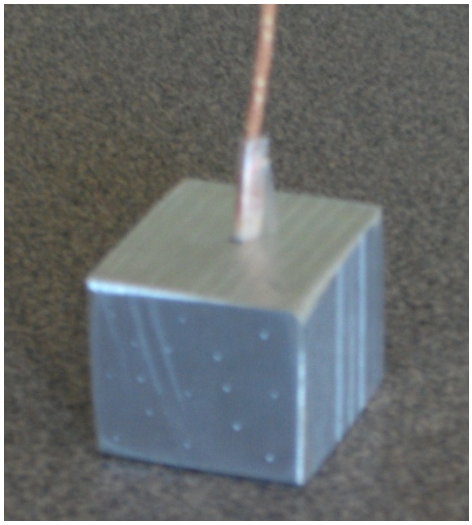

Figure 16: The thermocouple is secured with the aluminum block to secure the thermocouple in place during the furnace survey.

A single hole was drilled into the center of the aluminum blocks into which the thermocouples were inserted. The hole was only drilled half way through the block in order to measure the internal temperature of the block. By measuring the internal temperature opposed to the exterior temperature it allowed for a more even and consistent temperature measurement. To prevent the

thermocouples from loosening or falling out of the block, once the thermocouple was inserted a center punch was used to deform the opening of the hole and "pinch" the wire in place.

To ensure the thermocouples had made sufficient connection with the block, they were placed half way into ice water to see if the thermocouple would read the temperature of the block accurately. Given 30 minutes to reach equilibrium with the water, the thermocouples read the same temperatures which matched that of the water.

Testing the Solution Anneal Furnace

The aluminum blocks, once they had thermocouples inserted, were placed in chosen locations throughout the furnace. Six locations were chosen per test. The furnace was set for 995°F for the solution anneal temperature. Each test lasted about 5 hours to allow the blocks to reach equilibrium and to get a long enough recording of temperature fluctuations. For each position, the test was directed toward determining the peak temperature at that particular location along with the temperature variation over time. The furnaces had to meet a thermal stability of $\pm$10°F within a given position[10]. By determining the temperature gradients within the furnace, along with the locations of hot spots and cold spots, the preliminary samples could be placed into locations that would produce accurate solution anneal and the furnace set temperature could be adjusted so that the samples were at 995°F, not the furnace.

Testing the Low Temperature Ageing Oven

The low temperature oven was tested in a similar fashion as the furnace described above. However, the oven took considerably more time because the rack was adjusted up and down to find a height where the furnace had the smallest thermal gradients. Each test was only conducted

for 2 hours because the samples reached equilibrium more quickly than the high temperature furnace due to continuous air circulation by a fan within the oven.

Developing the Cooling Curves

Initial tests to create a cooling curve started with a solution anneal for 5 hours in the locations that were determined from the furnace testing. The samples were then removed from the furnace and air cooled while hanging from the thermocouple wire. The samples were quenched after specified intervals and the data was collected to determine the temperature drop associated with a particular quench delay time. However the data did not turn out well due to the short cooling time as well as the jostling of the samples which interfered with the thermocouple connection. This method did not provide sufficient results.

A second method was used for gathering the cooling curve data. The samples were solution annealed for about 5 hours and then removed from the furnace. The samples were cooled by hanging the samples in air off of a table edge. The samples were continuously cooled for 10 minutes until they were quenched. The results were clearer and curves were able to be fit to the data. Six samples were used to create cooling curves to determine the consistency of the cooling rate. The furnace room doors were remained closed during the cooling to prevent any air currents that would alter the test results.

Cooling curves were developed for the preliminary test samples and the flat tensile coupon samples. Preliminary samples were one inch cube blocks of aluminum 2219, similar to the blocks used to test the furnace. Because the cooling rate is largely dependent of the volume to surface area ratio, the tensile samples needed their own curve because they cooled at a faster rate than the blocks. Because the tensile samples are so thin and aluminum has such a high thermal

conductivity, the surface temperature was assumed to be similar to the internal temperature. In measuring the cooling curve for the tensile samples, the thermocouple was wrapped around the center of the gauge length so that it was in contact with the surface of the tensile sample. The samples were hung in the air to cool similarly to the block samples.

Preliminary Samples Heat Treatments

Heat treatments for the preliminary samples, 1 in. blocks, included a solution anneal at 995°F for 12 hours and a 26 hour age as specified in the ASM handbook. The furnace was set for 1025°F in order to heat the samples up to 995°F determined by the furnace testing. The samples were removed from the furnace and air cooled while hanging from the thermocouple wires. The quench delays used were 15, 25, and 35 seconds for initials testing. Longer quench delays of 55 seconds, 4 minutes, and air cooled (no quench) were used as comparisons. The samples were quenched into room temperature water, about 75°F, and the delay time was related to the material temperature from the cooling curve. The longer quench delay times were correlated to a temperature drop below 900°F and 750°F which were specific temperatures of interest. After the quench the samples were placed into an oven to age at 375°F for 26 hours. The samples were then water quenched.

Tensile Coupon Heat Treatments

The tensile samples were positioned in the furnace according to the furnace temperature survey results and solution annealed at 995°F for 12 hours. The samples were placed on top of ceramic risers to allow for quicker and easier removal from the furnace (Figure 17). The samples were air cooled and water quenched with quench delays of 5, 10, 15, 20, and 25 seconds. The quench water was at room temperature of about 75°F. The quench delays were related to the material

temperature using the cooling curve. The samples were then aged in the oven at 375°F for 26 hours. The samples were removed and water quenched.

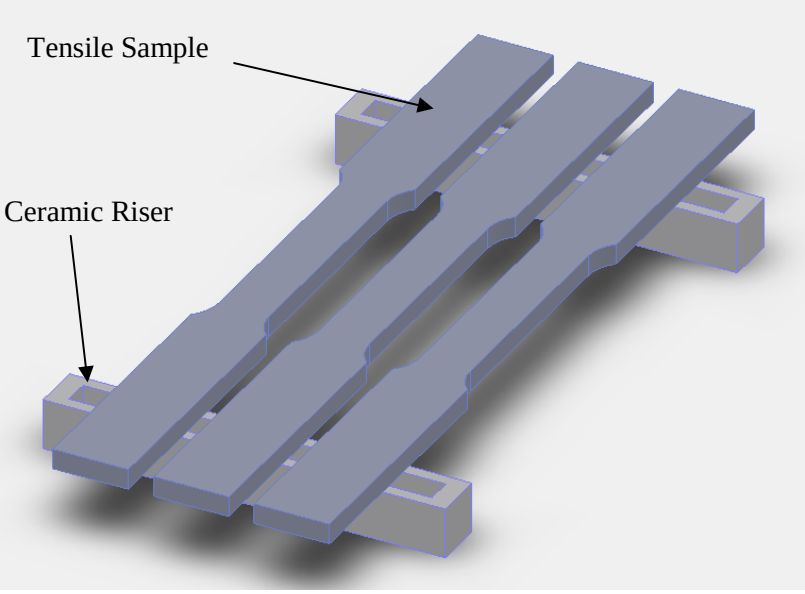

Figure 17: The tensile samples were positioned onto ceramic risers to allow for easier removal from the furnace.

Hardness Testing of Preliminary Samples

The preliminary samples could not be tensile tested because they were blocks. However, to get an idea of the heat treatment response for the different quench delays, hardness testing was used to determine differences between the samples. Rockwell B scale was used for the samples that were solution annealed and aged. Rockwell F was used on the solution anneal and water quenched sample along with the samples that was solution annealed and air cooled. The HRB scale was producing low to negative values on the softer samples that had not been aged so HRF was used. The hardness values of the heat treated samples and air cooled samples were compared to look for tends in the heat treatment response. Before the samples were tested they were smoothed using a 150-grit belt sander and hand finished with 600-grit sandpaper. Each block was tested on the same face 15 times to get a good distribution of data points.

Tensile Testing

The tensile samples were tested using an Instron with a 50 kN load cell. The samples were tested using a 1.5 mm/min crosshead displacement rate for the first three percent strain then it was increased to 3 mm/min until fracture. The samples were tested in groups according to the quench delay time. A 25.4 mm extensometer was used to record the beginning strain for Young's modulus. The extensometer was removed after 2.75 % strain which allowed the yield strength to be found at 0.2 % offset. The tensile strength, ductility, yield strength and Young's modulus were recorded and compared for all the tensile samples.

Metallography

The preliminary samples were used for metallographic imaging and analysis to determine if the quench delay affected the microstructure. The samples were not placed into a polymer mount, but remained as whole blocks. Polishing was done according to standard practices up to 0.5 micron using a diamond solution then etched using Kroll's reagent. The different quench delays were examined to see if the longer quench delays would increase the amount of the second phase ($CuAl_2$) present within the alloy. The precipitates are too small to see with optical microscopes so metallography was done to see how the second phase region was affected by the delay such as distribution and overall content. The aged samples were compared to the solution-anneal-air-cooled and solution-anneal-water-quenched samples to determine any differences.

Results

Furnace Testing

The data collected from the thermocouples during the furnace tests was used to find the positions within the furnace that had stable temperatures and would heat the 2219 alloy to the proper temperature (Figure 18). The furnaces needed to meet a minimum thermal stability of ±10°F for the heat treatment of the aluminum. The furnace temperature was set to 1020°F and the target solution anneal temperature of the 2219 alloy was 995°F. Over a period of twenty hours there was a thermal stability of about ±2-3°F. However the thermal gradients within the furnace were significant. The furnace had temperature gradients of about 20°F from the front center to back corner of the furnace. Two samples were placed only a few inches apart showed temperature differences of about 10°F.

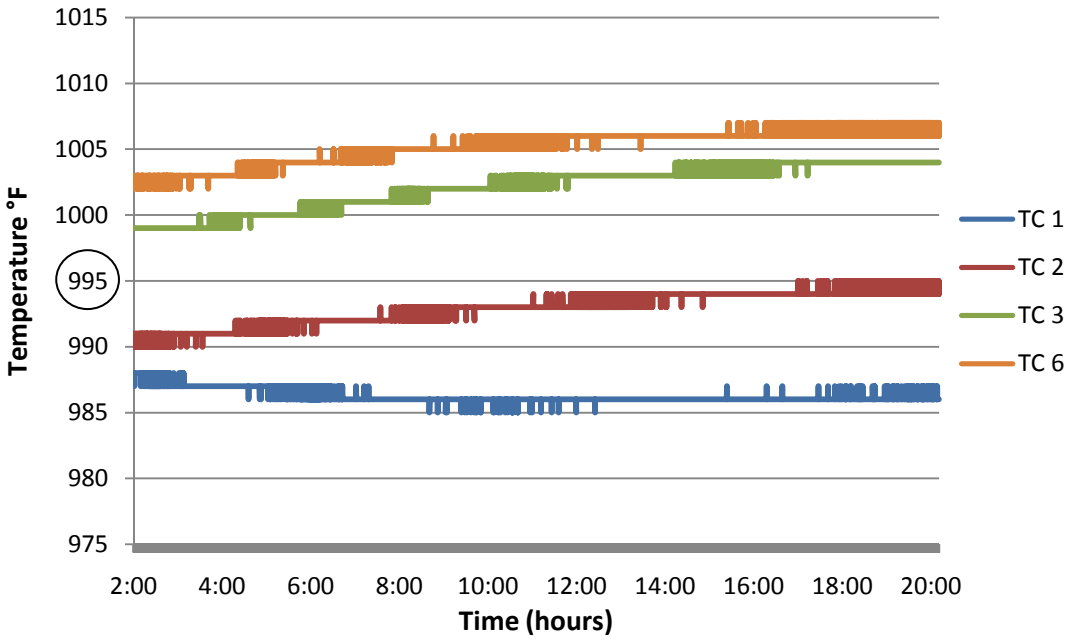

Figure 18: The thermocouple data shows the thermal gradients within the furnace and the temperature fluctuations at a particular position. TC referes to the thermocouple and position within the furnace.

Cooling Curves

The preliminary samples were continuously cooled for about 10 minutes with thermal measurements recorded every second. The data points were graphed in Excel and a trend line was fit to the curve (Figure 19). The equation of the trend line was used to correlate the quench delay to the alloy temperature at the quench. A few iterations of developing the cooling curves were done to ensure repeatability of the cooling rate and the consistency of cooling between batches. The cooling rate was fairly consistent between samples with the exception of the starting temperature of the material. Depending on where the samples were in the furnace they started at different temperatures when removed for cooling.

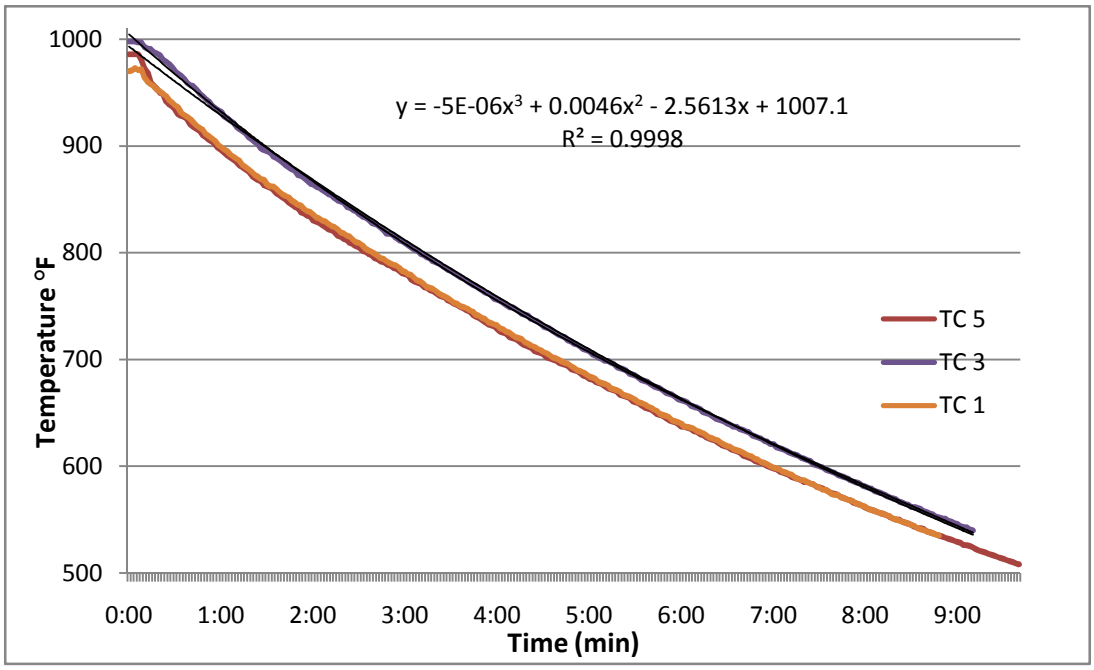

Figure 19: The cooling curve of the preliminary block samples were used to correlate the quench delay time to the material temperature. TC represents the location in the furnace and in the room the sample was placed for cooling.

Separate cooling curves were generated for the tensile samples because they cooled more quickly than the aluminum blocks (Figure 20). The method of cooling the samples is primarily convection and a little radiation for heat transport. Because the surface area of the tensile

samples is greater than the surface area of the blocks, there was more surface area exposed to the air for convection and radiation to occur. Because of the increased convection and radiation heat could be dissipated quicker and with less mass to cool as well there was less overall energy to dissipate. The combination of less overall energy and quicker energy dissipation led to faster cooling rates. Shorter quench delays were used for the tensile coupons because of the increased cooling rate.

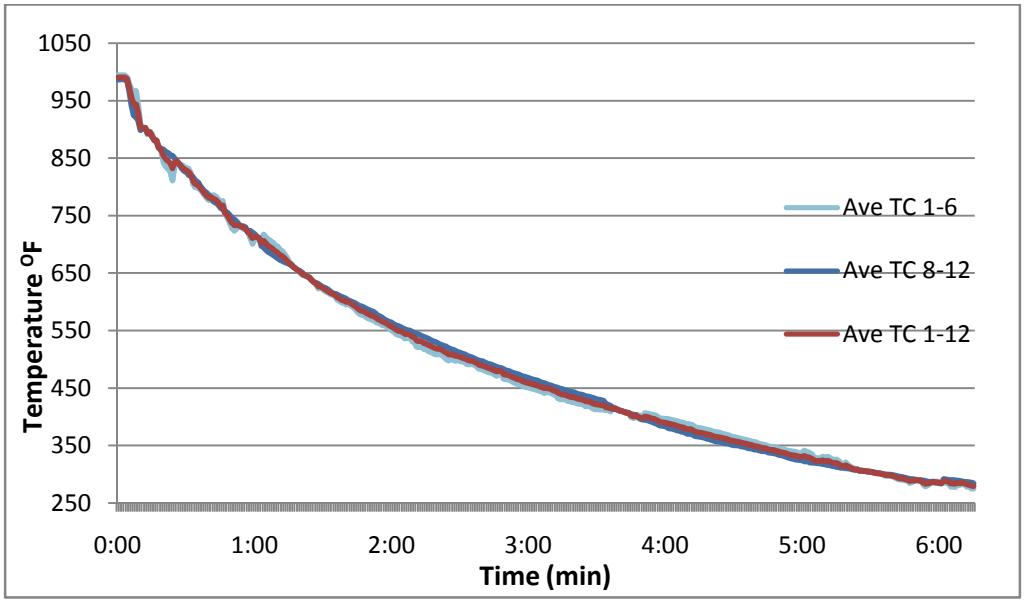

Figure 20: Twelve tensile samples were cooled and the individual cooling curves were averaged together to produce a uniform curve.

The part of the cooling curve that was important was the first few minutes. Because the goal was to see how a 15 second delay affects the alloy, the graph was shortened to focus on the initial time delay verse temperature drop region of the curve (Figure 21). A trend line was used to fit the data and relate the time and temperature for the tensile coupons. The equation of the trend line was used to calculate an approximate alloy temperature for a given quench delay time.

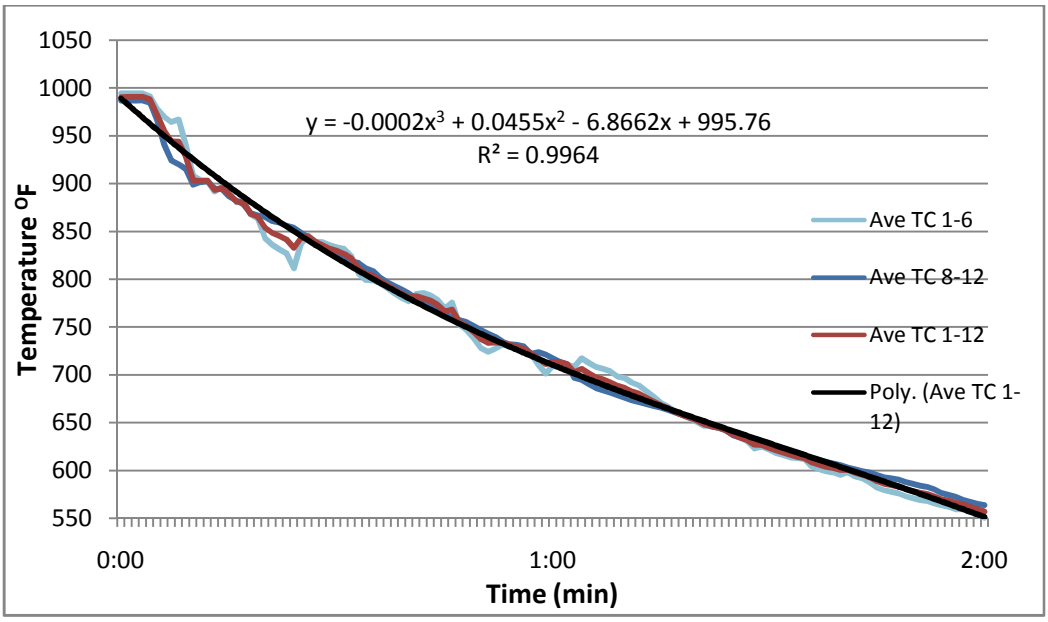

Figure 21: A trend line was fit to the first 2 minutes of the cooling curve from Figure 20.

Preliminary Hardness Data

Hardness testing was performed on preliminary samples as-received and with varying quench delays. The hardness data collected from the heat treated samples was compared to the data recorded from the samples received from Weber Metals (Figure 22). There was no apparent trend correlating quench delay to hardness because samples with longer quench delays had higher hardness than samples with shorter quench delays in some cases. The as-received samples were used as a control group to determine the effects of heat treatment and to determine similarities to Weber Metals' current results.

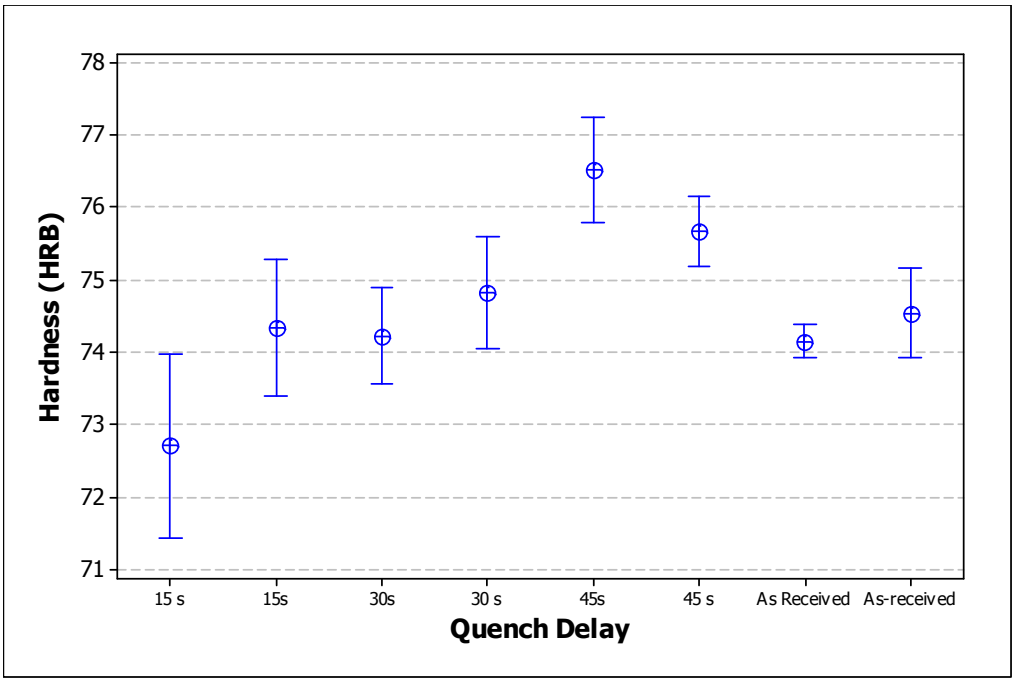

Figure 22: The samples were categorized by their quench delays to compare the average hardness and scatter within each group. The interval shows the 95% confidence interval of the mean for the group.

ANOVA statistical analysis was used to compare the hardness data from the different samples and look for significant differences and trends. The typical hardness of the samples ranged around 72-76 HRB. There were no trends found from the ANOVA analysis but there were some significant differences (Appendix A). Tukey Kramer comparisons were used to determine similarities between groups. The samples that had significant differences were highlighted. Multiple comparisons were performed to see how the significant differences changed as samples were added and removed from the comparison. The significant differences between samples did change as quench delays were removed.

Because there were no noticeable trends in the samples tested, longer quench delays were used to determine if more noticeable decreases in the hardness would occur. A 55 second and a 220 second quench delay was used which corresponded to a material temperature of 900°F and 750°F (Figure 23). There was a noticeable drop in hardness for the samples with a 220 second

delay. These temperatures were investigated because research showed that these two temperatures were considered crucial temperatures in the heat treatment response. According to MIL-H-6088 the material should remain above 400°C (750°F). However, hardness data showed that this length of time and temperature produces values much lower than the shorter quench delays. The drop in hardness may be a result of the longer cooling because more Cu could diffuse out of solution reducing the amount of Cu available to precipitate as θ or θ' during ageing.

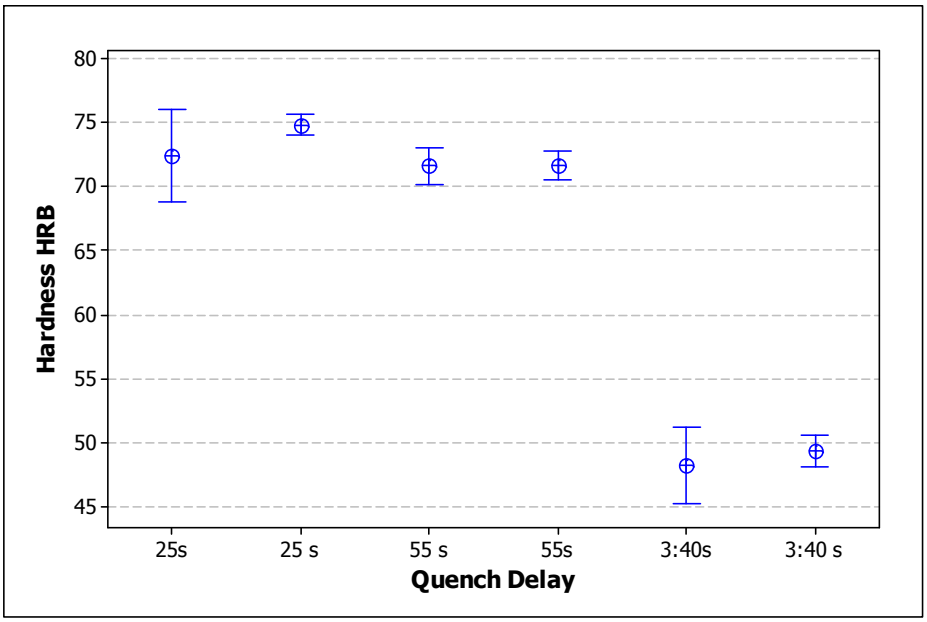

Figure 23: A significant difference in hardness was seen for a much longer quench delay time.

To ensure the heat treatment was working properly, hardness tests were performed on solution annealed samples that were water quenched with a 5 second quench delay (Figure 24). The hardness values were much lower than the T6 condition samples around 36-38 HRB. Also, because aluminum can be strain hardened relatively easy, the hardness was taken after the samples were quenched and also after the samples were cut to size and sanded smooth (post preparation - PP). The preparation of the samples increased the average hardness, but not enough

to make any statistical difference. Because the surface preparation of the samples did seem to affect the samples, even though there was no statistical effect, the samples were prepared as much as possible prior to heat treating so that the added effects of strain hardening would not affect the quench delay hardness testing.

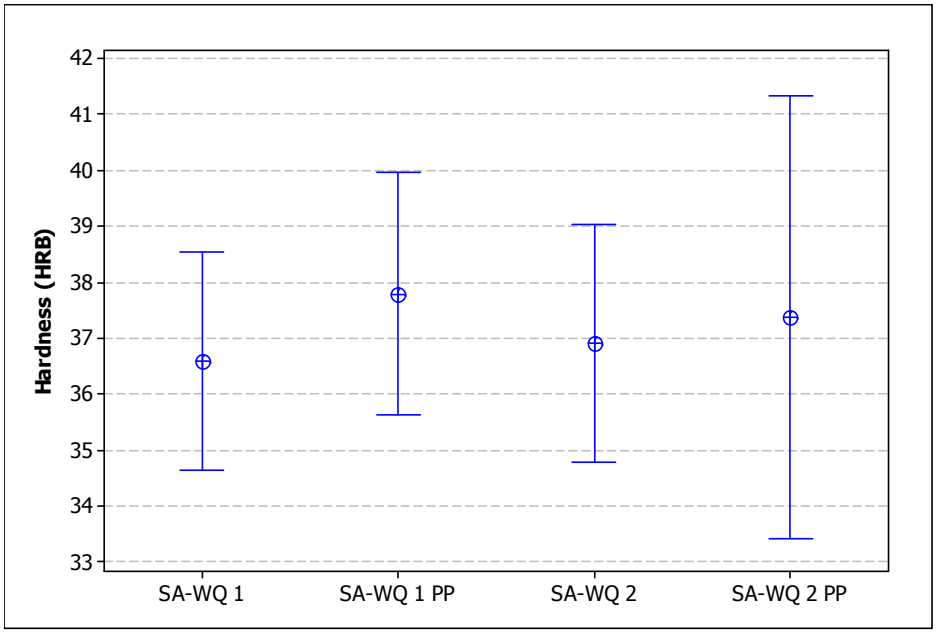

Figure 24: The samples were tested for hardness after a solution anneal (SA) and water quenched (WQ) to determine the ageing effects. Samples were also tested for the effects of strain hardening which may have resulted from preparing the sample (PP).

Hardness tests were conducted on 1 in. blocks that were solution annealed and allowed to air cool (AC) (Figure 25). This acted, essentially, as a long quench delay and the microstructure and hardness was recorded to determine the effects. This test was also used to quantify the effects of ageing on the hardness when the samples were not water quenched after being removed from the furnace. There were significant differences in hardness between the two samples SA-AC 1 and SA-AC 2. The difference in hardness between the two samples was attributed to cooling rate. Though both samples were air cooled, sample SA AC 2 was about 5 times larger in mass than SA AC 1. Because of the difference in mass, the samples cooled at different rates which may be

the cause of the hardness differences. The larger samples cooled at a slower rate than the smaller sample. Slower cooling allows for more alloying elements to diffuse out of solution and a courser second phase. Less alloying elements in solution results in reduced strain, which lowers the strength and hardness of the material. These samples were also used to investigate the effect that sample preparation had on the hardness. Hardness was measured on the samples before and after the surface preparations. There were no statistically significant effects on hardness between the AC and PP samples due to strain hardening. However, there was an increase in the average hardness of the material as seen previously.

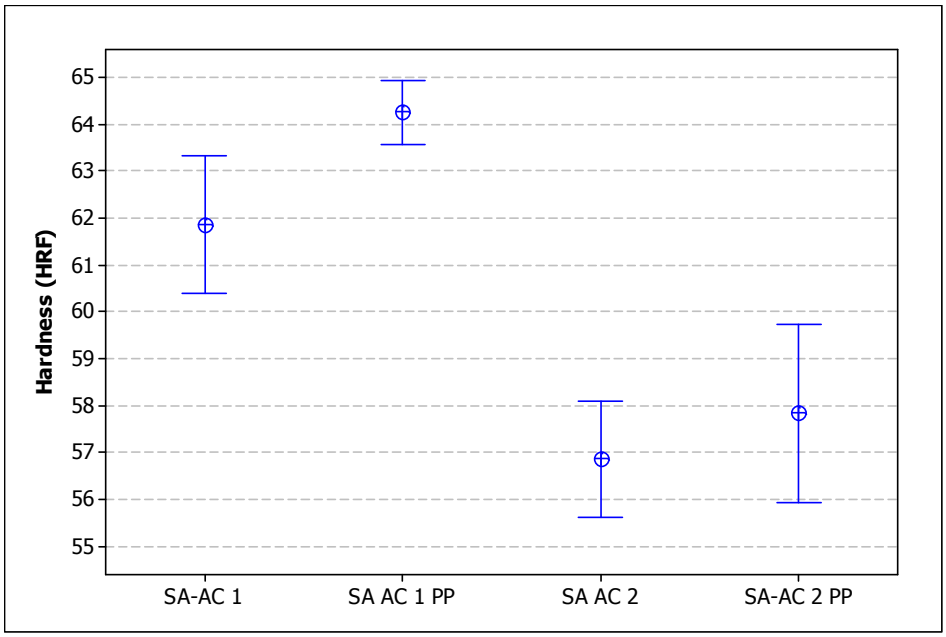

Figure 25: Air cooled samples were used to investigate how the material would respond to ageing without the use of a water quench. The hardness was measured in HRF because the material was too soft to use the HRB scale.

Tensile Testing

Tensile tests were done on 5 samples for each quench delay (QD). The tensile strengths were compared to find significant differences and trends between the quench delay times (Figure 26). The tensile stress-strain curves can be seen in Appendix B. There were no statistical differences

between the QDs, but there did appear to be a trend of decreasing tensile strength with increased quench delay. Because the sample size was so small, only 5 samples each, the power of each comparison was low. In order to have more reliable comparisons, more samples would be necessary for each QD time. The tensile strength data ranged from around 395-435 MPa with average tensile strengths around 405-425 MPa. The statistical comparison data for the tensile strength data is located in Appendix C. The data shows the pairwise comparisons of the ANOVA testing and shows that there was no statistical difference between the samples.

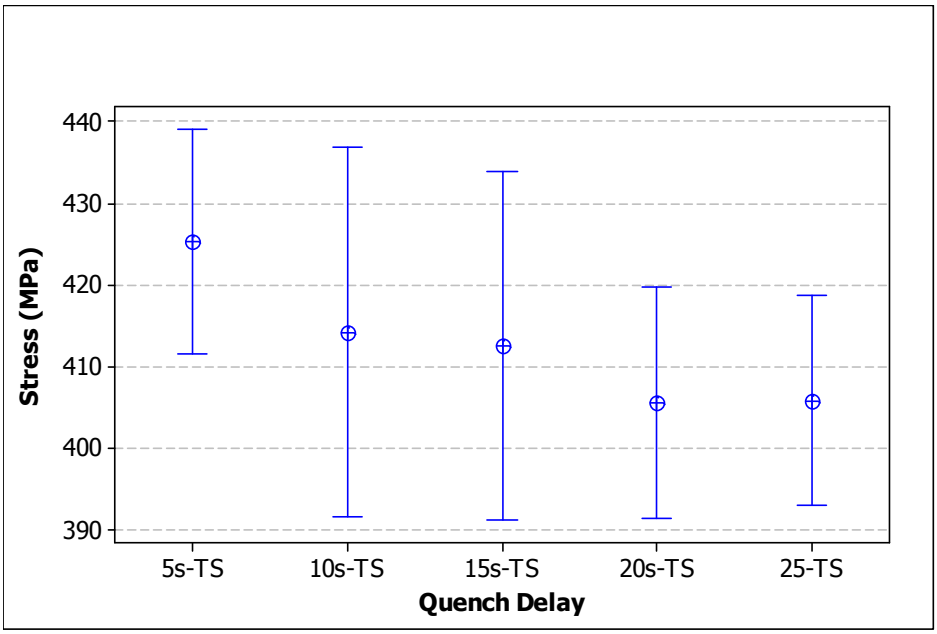

Figure 26: When comparing the tensile strength of the samples there were no statistical differences, but there appeared to be a trend of decreasing strength with increasing QD.

The yield strength of the samples were determined at 0.2% offset and compared between QDs (Figure 27). An ANOVA test was performed on the data to determine differences in the data (Appendix C). The results of the ANOVA showed no significant difference between the different QD groups. However, a trend was apparent of decreasing yield strength with increasing QD. If the number of samples for each quench delay was increased then the results would be more reliable. Because there was only a few samples tested and there was so much scatter in the results

the standard deviation was increased along with the 95% confidence interval. With such large ranges, it is difficult to determine true differences between the tests. However, the average yield strength did decrease as the quench delay increased. The average yield strength ranged from about 280-300 MPa.

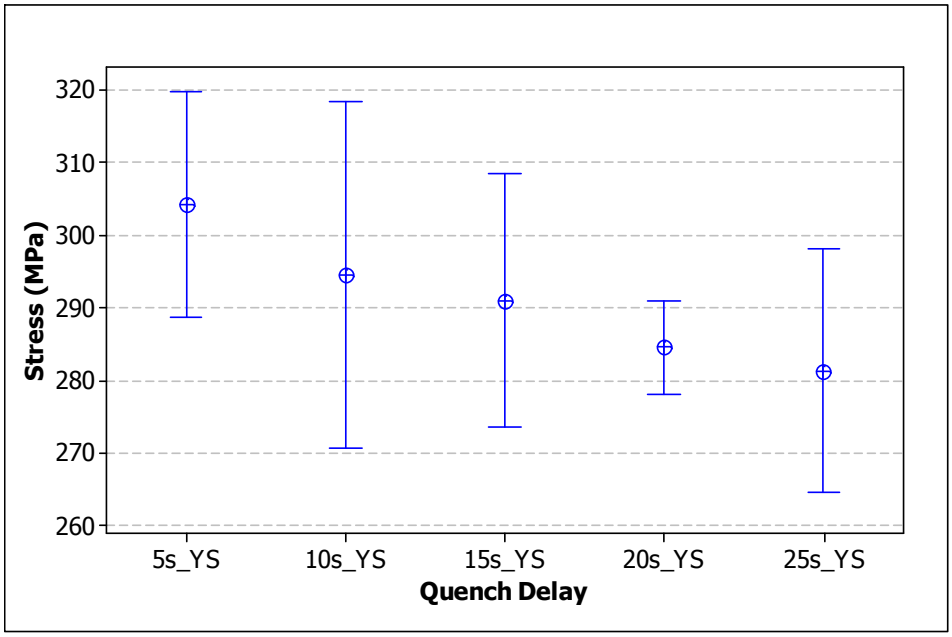

Figure 27: The yield strengths appear to be decrease as the QD increases, however, no statistical differences were observed.

The tensile data is presented in Table II which shows the average strength and the standard deviation for each group of samples. There was a large scatter in the tensile and yield strengths for the 10 and 15 second QD groups. The scatter in the 25 second QD group was about the same for both yield strength and tensile strength. The stress-strain curves from the tensile testing can be seen in Appendix B and are organized by quench delay. There were few noticeable differences in the tensile behaviors of the samples between quench delay groups.

Table II: Tensile Data of Al 2219

Quench Delay (s)	Average TS (MPa)	Standard Deviation (MPa)	Average YS (MPa)	Standard Deviation (MPa)	Material Temperature (°F)
5	425.28	11.05	304.25	9.81	962
10	414.18	18.25	294.50	15.02	931
15	412.54	17.16	291.00	10.95	902
20	405.58	11.39	284.50	4.04	875
25	405.83	10.41	281.25	10.56	850

To pass the quality inspection the samples needed to meet a minimum required tensile strength of 400 MPa and yield strength of 276 MPa. Seven of the tested samples failed to meet the tensile strength requirements: one 10s, one 15s, two 20s, and three 25s samples, the ##s refer to the quench delay time. Only one sample, which had undergone a 25 second quench delay, failed to meet the yield strength requirement of 276 MPa. However, a few samples passed the yield strength requirement with strengths of about 278 MPa. One trend that developed was that the yield strength and tensile strength consistently had a difference of about 115-120 MPa regardless of the quench delay.

Metallography

Metallography was performed on the preliminary testing blocks to examine microstructural changes within the material as the quench delay was increased. In a solution annealed sample with a 5 second quench delay that had not been aged there were several areas of concentrated $CuAl_2$ (Figure 28).

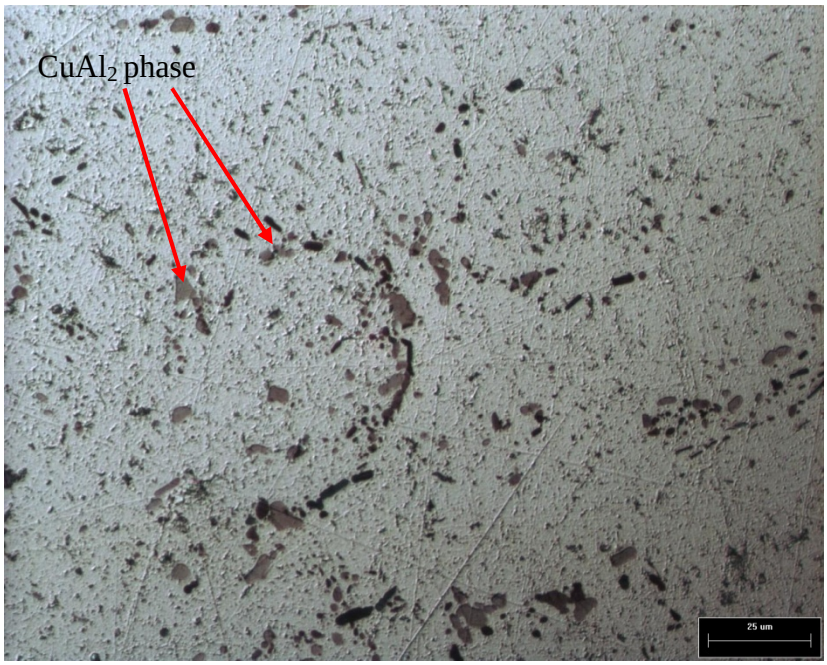

Figure 28: A solution annealed sample with a 5 second quench delay had large regions of $CuAl_2$ primarily around the grain boundaries. Etched using Kroll's reagent.

A 10 second quench delay sample was aged to see how the microstructure changed during the heating process (Figure 29). The sample showed less overall regions of $CuAl_2$ and what was present was dispersed more evenly. This is because the $CuAl_2$ is mostly in solution or dispersed as a fine precipitates throughout the solvent material.

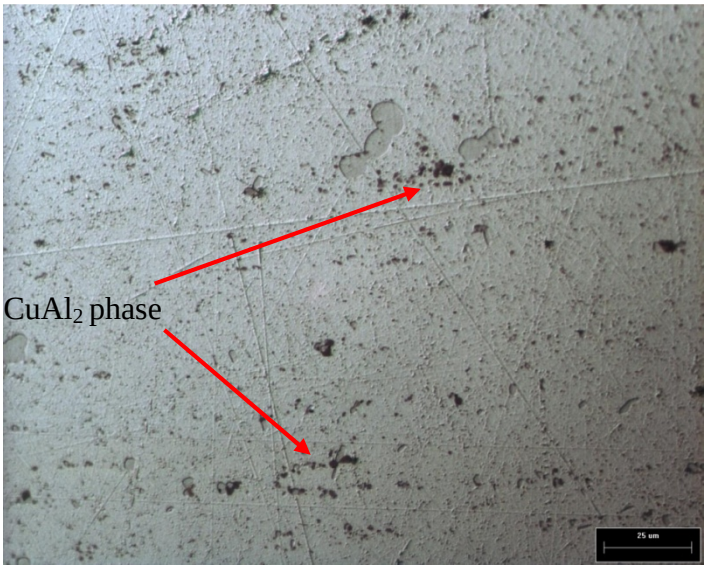

Figure 29: A sample with a 10 second quench delay had few regions of concentrated $CuAl_2$. Etched using Kroll's reagent.

Longer quench delays were thought to allow for more $CuAl_2$ to diffuse out of solution as the material cools and the solubility limit decreases. When a 55 second quench delay sample was examined, it showed much more $CuAl_2$ regions than a 10 second delay sample (Figure 30). As more Cu diffused out of solution it increased the amount of $CuAl_2$ that formed. The 55 second delay was approximate to cooling the material to 900°F which allowed for diffusion but not much time for growth of the second phase regions.

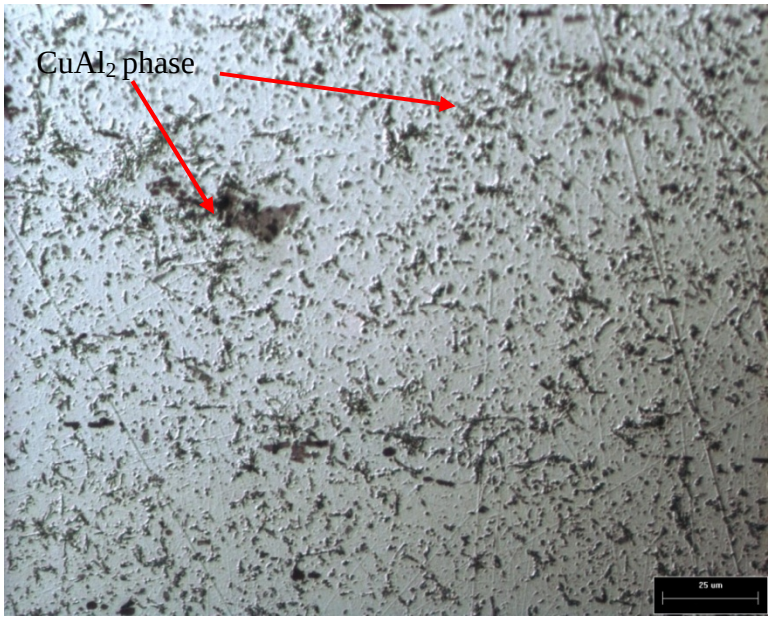

Figure 30: A 55 second quench delay sample showed increased amounts of $CuAl_2$ regions compared to the 10 second delay sample. The darker regions are the second phase regions which form as the solubility of Cu decreases as the material cools. Etched using Kroll's reagent.

As the quench delay was increased the amount of $CuAl_2$ that formed seemed to have increased a small amount but the distribution was the major difference (Figure 31). At a longer quench delay of about 220 seconds the sample cooled to about 750° F. Because of the high temperature and long time period the Cu was able to diffuse out of solution but it also had time to diffuse into large precipitate regions. With the longer quench delay there were increased sized regions of $CuAl_2$ as the precipitates were able to grow together.

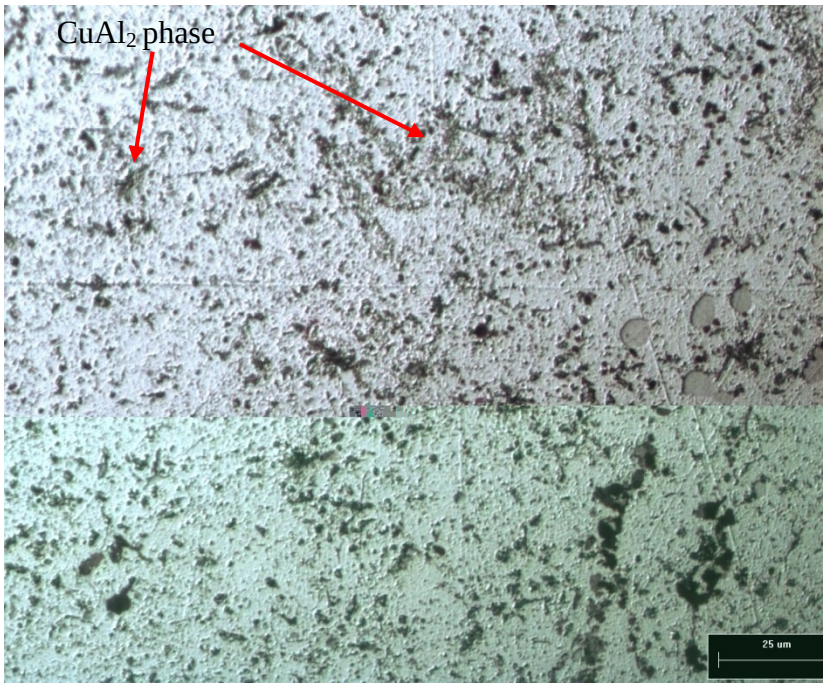

Figure 31: A sample with a quench delay of 3 min 40 seconds showed an increase in the amount of $CuAl_2$ and particle growth of the precipitates. Etched using Kroll's reagent.

Because the precipitates that strengthen the material are submicron in size, a transmission electron microscope (TEM) is necessary to see them. Because the precipitates cannot be seen using metallography the drop in hardness of the 220 second delay can only be correlated to having less Cu in solution to form $CuAl_2$ precipitates. If a TEM was used to look at the precipitates, the hardness changes could be correlated to changes in the precipitate development process.

Discussion

Hardness Testing

The macrohardness testing did not show any trends in the hardness data. One sample that had a 15 second quench delay was significantly lower than another sample with a 15 second quench delay. The samples that had the highest strength had a 35 second delay which was expected to be

lower than a 15 second delay. The samples also showed high amounts of scatter with standard deviations of 10-17 HRB. Causes for the scatter and inconsistent hardness values between all the samples were investigate. The location of the samples in the furnace was the first cause investigated. It was a possibility that the quench delays produced inconsistent hardness values because the sample with a 15 second delay could have been cooler than a sample with a 25 second delay if the 15 s sample was cooler than the 25 s sample when removed from the furnace. However, this would not have explained how a 35 second quench delay would be stronger than a 15 second delay, unless the 15 s samples were significantly less hot to begin. When I looked back at the furnace testing there were no positions in the furnace that had a temperature difference great enough to explain how a 35 second delay would be hotter than a 15 second delay at the quench. The differences between the samples were only about 10°F during the solution anneal.

The next possibility investigated was the ageing temperature of the sample. The 15 second delay sample could have been either overaged or underaged depending on the temperature of the part in the oven. If the part was too far below the ageing temperature of 375°F, the precipitates may not have developed enough to properly strengthen the material. Because the diffusion of Cu in the Al matrix is temperature dependant, a small change in temperature can have a large effect on the diffusion rate. Likewise, if the part was too hot then the precipitates may have over developed which reduces the strength of the material. At higher temperatures Cu diffuses faster, increasing the rate at which the $CuAl_2$ precipitates form and grow. In order for the precipitates to strengthen the material they must be dispersed enough throughout the material to reduce dislocation motion. If the particles are too small then the dislocations can move through or around the precipitates' stress field. If the particles are too large and not dispersed as well the

dislocations can move around them. When I looked back at the thermal profiles for the heat treated samples, none of the samples were more than $\pm$6°F from the 375°F ageing temperature. The specific samples, 15s and 35s, that showed the greatest difference in hardness, were aged at 374 and 373°F respectively; a one degree difference during aging would not explain the large differences in hardness. The differences in hardness may be link to the precipitates, but to truly determine how the precipitates differ between the samples; a TEM would need to be used to view the size and distribution of the precipitates within the Al matrix. This seems to be the most likely explanation of the hardness differences, however, it cannot be proved without knowing the differences in the precipitates between the samples.

Other possibilities of error could have been caused by the hardness tests itself. Because the hardness test is a localized measurement to correlate a material's bulk property, there could be differences within the samples locally which can affect the results. This is why hardness tests are generally performed over a range of areas to get an average of the material properties. This could explain why some samples had small scatter and other had higher scatter as well as why the hardness data had higher standard deviations than the tensile testing data. But, this does not explain why the average hardness of the samples was so different and why a longer quench delay was harder than a shorter quench delay.

Tensile Testing

The tensile testing results showed a decreasing trend of tensile strength and yield strength as the quench delay increased. This was the expected trend because with longer cooling times more Cu is able to diffuse from solution. If less Cu is in solution, when the alloy is aged there is less Cu available to diffuse out into $CuAl_2$ precipitates which reduces the amount of precipitation

hardening. With less Cu to form precipitates they would not be as finely dispersed within the alloy which is a key factor for precipitation hardening. However, in order to see how the precipitates differ between the samples, a TEM would need to be used to determine the distribution and size characteristics of the precipitates.

When the samples were checked to see which would pass the quality inspection more samples failed the tensile strength requirement than the yield strength requirement. This makes sense because based on the data collected the tensile and yield strength differed by about 115 MPa. The quality inspection had a 125 MPa difference between the tensile and yield strength which means that a sample could fail the tensile strength requirement and still pass the yield strength. The correlation between the tensile strength and yield strength seen in the data can be an effect of the precipitates and the matrix material or simply an effect of the testing set up.

Some interesting results though were why the hardness data did not show a correlation between the quench delay and the tensile data did. One possibility is if the samples were not flat during the hardness testing, the indenter could have slipped creating the appearance of a softer material. However, the inconsistencies in the hardness data were expected, which was the reason for preparing and testing tensile coupons.

Looking at the trend of the tensile strength data, the average strength values begin to approach 400 MPa around a quench delay of 25 seconds. If the scatter in the material property could be reduced to produce more consistent tensile properties by using tighter control on the heat treatment, then as suggested by the tensile strength data, as long at the material is above about 850°F at the quench the sample should respond to the heat treatment and still pass quality. This provides a lower limit to the material temperature that will result in acceptable properties. The 15

second delay that is specified by manufacturing specification MIL-H-6088 probably uses a safety factor to account for potential scatter within the production line so that even the samples with lower strength will still be above 400 MPa. The 850°F limit is right on the lower limit of the temperature because, in average, the material will pass inspection. However, if there is any amount of scatter in the material properties the material could easily fail inspection, resulting in having to re heat treat the material.

Conclusions

1. Increasing the quench delay results in decreasing strength of the alloy.
2. A 25 second delay produces acceptable properties.
3. A alloy temperature of 850°F or greater should produce acceptable properties.
4. Small sample sizes limited the statistical effects between quench delays due to large scatter in the data.

Acknowledgements

I would like to thank Weber Metals for their support with the project. Their support with materials and intellectual assistance helped to make the project possible. I would also like to thank Cal Poly Material Engineering Department for use of testing equipment and lab space. I would like to thank Blair London and his senior project group for their assistants.

References

[1] Hartman JA, Beil RJ, Hahn GT Effect of copper rich regions on tensile properties of VPPA weldments of 2219-T87 Aluminum Alloy. Weld Journal 1987 V 66:73s–83s

[2] ASM Handbook. Volume 2, In *Properties and Selection: Nonferrous alloys and special purpose materials.* ASM, 2002 Online

[3]ASM Handbook. Aluminum and Aluminum Alloys: Fabrication and Finishing of Aluminum Alloys, Heat Treating, 1993 Pg 300

[4] ASM Handbook. Aluminum and Aluminum Alloys: Fabrication and Finishing of Aluminum Alloys, Heat Treating, 1993 Pg 296

[5] ASM Handbook. Volume 4, Heat Treating: Heat Treating of Aluminum Alloys, Precipitation from Solid Solution. ASM, 2002 Online

[6] ASM Handbook. Volume 4, Heat Treating: Heat Treating of Aluminum Alloys, Strengthening by Heat Treatment. ASM, 2002 Online

[7] Coriell, S. Precipitation Hardening of Metal Alloys: < http://nvl.nist.gov/pub/nistpubs/sp958-lide/014-015.pdf>

[8] McMahon, C.J. Jr. Structural Materials. Merion Books, Philadelphia, PA. 2004. Print

[9] McMahon, C.J. Jr. Structural Materials. Merion Books, Philadelphia, PA. 2004. CD ROM

[10] ASM Handbook. Aluminum and Aluminum Alloys. Fabrication and Finishing of Aluminum Alloys, Heat Treating, 1993 Pg 292

[11] AluMatter. Strengthening Mechanisms, Precipitation Hardening. 2009. <http://aluminium.matter.org.uk/content/html/eng/default.asp?catid=71&pageid=-1855656659>

[12] ASM Handbook. Aluminum and Aluminum Alloys: Fabrication and Finishing of Aluminum Alloys, Heat Treating, 1993 Pg 303

[13] ASM Handbook. Aluminum and Aluminum Alloys: Fabrication and Finishing of Aluminum Alloys, Heat Treating, 1993 Pg 311

[14] Kawata, H., K. Sakamoto, T. Moritani, S. Morito, T. Furuhara, T. Maki. Crystallography of Ausformed Upper Bainite Structure in Fe–9Ni–C Alloys. Materials Science and Engineering: A. Volumes 438-440, 2006, Pages 140-144

[15] D.A. Porter and K.E. Easterling, *Phase Transformations in Metals and Alloys,* 2nd ed., Chapman and Hall, 1996, p 514

[16] ASM Handbook. Aluminum and Aluminum Alloys: Fabrication and Finishing of Aluminum Alloys, Heat Treating, 1993 Pg 291

[17] ASM Handbook, Volume 9, Metallography and Microstructures: Structures by Precipitation from Solid Solution, 2004 pg 135

[18] W.H. Van Geertruyden, W.Z. Misiolek, G.G. Lea, and R.M. Kelly, Thermal Cycle Simulation of 6xxx Aluminum Alloy Extrusion, *Proc. Seventh International Extrusion Technology Seminar* (Chicago, IL) Aluminum Extruders Council, 2000

[19] Han, Chung-Souk , R. H. Wagoner, F. Barlat. On Precipitate Induced Hardening in Crystal Plasticity: Theory. International Journal of Plasticity. Volume 20-3, 2004, Pages 477-494

[20]ASM Handbook. Volume 8, Mechanical Testing and Evaluation: Introduction to the Mechanical Behavior of Nonmetallic Materials, Deformation/Strengthening Mechanisms. ASM, 2002 Online

[21] Douin, J., P. Donnadieu, T. Epicier, G.F. Dirras, A. Proult, J.F. Silvain. Stress field Around Precipitates: Direct Measurement and Relation with the Behavior of Dislocations. Materials Science and Engineering. A319–321 2001 270–273

[22] CES EduPack 2009 software, Granta Design Limited, Cambridge, UK, 2009.

Appendix A: Statistical Comparisons of Hardness Data

One-way ANOVA: Preliminary Samples Hardness Data

```
       Source   DF        SS       MS       F      P
       Factor   11  16225.16  1475.01  294.09  0.000
       Error   168    842.60     5.02
       Total   179  17067.76
       S = 2.240   R-Sq = 95.06%   R-Sq(adj) = 94.74%
Individual 95% CIs For Mean Based on Pooled StDev
Level    N    Mean  StDev    -+---------+---------+---------+--------
15 s    15  72.713  2.277                                  (-*)
15s     15  74.347  1.707                                     (*)
25s.    15  74.227  1.208                                   (-*)
25 s    15  74.827  1.400                                    (-*)
35s     15  76.520  1.294                                      (-*)
35 s    15  75.673  0.878                                     (-*)
55 s    15  71.600  2.584                                 (-*)
55s     15  71.660  2.026                                 (-*)
3:40s   15  48.247  5.363    (*-)
3:40 s  15  49.420  2.292     (-*)
AR      15  74.153  0.414                                   (-*)
AR.     15  74.540  1.119                                    (*-)
                           -+---------+---------+---------+--------
                         48.0      56.0      64.0      72.0

Pooled StDev = 2.240
Tukey 95% Simultaneous Confidence Intervals
All Pairwise Comparisons
Individual confidence level = 99.89%
15 s subtracted from:
          Lower   Center    Upper  ---------+---------+---------+---------+
15s      -1.079    1.633    4.345                   (-*-)
25s.     -1.199    1.513    4.225                   (-*-)
25 s     -0.599    2.113    4.825                    (*-)
35s       1.095    3.807    6.519                     (*-)
35 s      0.248    2.960    5.672                    (-*-)
55 s     -3.825   -1.113    1.599                 (*-)
55s      -3.765   -1.053    1.659                 (*-)
3:40s   -27.179  -24.467  -21.755    (-*)
3:40 s  -26.005  -23.293  -20.581     (*-)
AR       -1.272    1.440    4.152                   (-*-)
AR.      -0.885    1.827    4.539                   (-*-)
                                   ---------+---------+---------+---------+
                                          -16         0        16        32

15s subtracted from:
          Lower   Center    Upper  ---------+---------+---------+---------+
25s.     -2.832   -0.120    2.592                 (-*-)
25 s     -2.232    0.480    3.192                  (*-)
35s      -0.539    2.173    4.885                   (*-)
35 s     -1.385    1.327    4.039                  (-*-)
```

```
55 s     -5.459   -2.747   -0.035                 (*-)
55s      -5.399   -2.687    0.025                 (*-)
3:40s   -28.812  -26.100  -23.388   (-*)
3:40 s  -27.639  -24.927  -22.215    (*-)
AR       -2.905   -0.193    2.519                  (-*-)
AR.      -2.519    0.193    2.905                  (-*-)
                                   ---------+---------+---------+---------+
                                          -16         0        16        32
```

25s. subtracted from:

```
          Lower   Center    Upper  ---------+---------+---------+---------+
25 s     -2.112    0.600    3.312                   (*-)
35s      -0.419    2.293    5.005                    (*-)
35 s     -1.265    1.447    4.159                   (-*-)
55 s     -5.339   -2.627    0.085                 (*-)
55s      -5.279   -2.567    0.145                 (*-)
3:40s   -28.692  -25.980  -23.268   (-*)
3:40 s  -27.519  -24.807  -22.095    (*-)
AR       -2.785   -0.073    2.639                  (-*-)
AR.      -2.399    0.313    3.025                   (*-)
                                   ---------+---------+---------+---------+
                                          -16         0        16        32
```

25 s subtracted from:

```
          Lower   Center    Upper  ---------+---------+---------+---------+
35s      -1.019    1.693    4.405                   (-*-)
35 s     -1.865    0.847    3.559                   (-*)
55 s     -5.939   -3.227   -0.515                (-*-)
55s      -5.879   -3.167   -0.455                (-*-)
3:40s   -29.292  -26.580  -23.868   (*-)
3:40 s  -28.119  -25.407  -22.695   (-*-)
AR       -3.385   -0.673    2.039                  (-*)
AR.      -2.999   -0.287    2.425                  (-*-)
                                   ---------+---------+---------+---------+
                                          -16         0        16        32
```

35s subtracted from:

```
          Lower   Center    Upper  ---------+---------+---------+---------+
35 s     -3.559   -0.847    1.865                   (*-)
55 s     -7.632   -4.920   -2.208               (-*-)
55s      -7.572   -4.860   -2.148               (-*-)
3:40s   -30.985  -28.273  -25.561  (*-)
3:40 s  -29.812  -27.100  -24.388  (-*-)
AR       -5.079   -2.367    0.345                  (-*)
AR.      -4.692   -1.980    0.732                  (-*)
                                   ---------+---------+---------+---------+
```

```
                                      -16         0        16        32


35 s subtracted from:

          Lower   Center    Upper  ---------+---------+---------+---------+
55 s     -6.785   -4.073   -1.361                (*-)
55s      -6.725   -4.013   -1.301                (*-)
3:40s   -30.139  -27.427  -24.715  (-*-)
3:40 s  -28.965  -26.253  -23.541   (-*)
AR       -4.232   -1.520    1.192                 (-*-)
AR.      -3.845   -1.133    1.579                  (*-)
                                  ---------+---------+---------+---------+
                                         -16         0        16        32


55 s subtracted from:

          Lower   Center    Upper  ---------+---------+---------+---------+
55s      -2.652    0.060    2.772                   (-*-)
3:40s   -26.065  -23.353  -20.641     (*-)
3:40 s  -24.892  -22.180  -19.468     (-*-)
AR       -0.159    2.553    5.265                     (-*)
AR.       0.228    2.940    5.652                     (-*-)
                                  ---------+---------+---------+---------+
                                         -16         0        16        32


55s subtracted from:

          Lower   Center    Upper  ---------+---------+---------+---------+
3:40s   -26.125  -23.413  -20.701     (*-)
3:40 s  -24.952  -22.240  -19.528     (-*-)
AR       -0.219    2.493    5.205                     (-*)
AR.       0.168    2.880    5.592                     (-*)
                                  ---------+---------+---------+---------+
                                         -16         0        16        32


3:40s subtracted from:

         Lower  Center   Upper  ---------+---------+---------+---------+
3:40 s  -1.539   1.173   3.885                   (-*)
AR      23.195  25.907  28.619                                 (-*-)
AR.     23.581  26.293  29.005                                  (*-)
                               ---------+---------+---------+---------+
                                      -16         0        16        32


3:40 s subtracted from:

      Lower  Center   Upper  ---------+---------+---------+---------+
```

```
AR   22.021  24.733  27.445                                  (*-)
AR.  22.408  25.120  27.832                                  (-*)
                            ---------+---------+---------+---------+
                                   -16         0        16        32


AR subtracted from:

      Lower  Center  Upper  ---------+---------+---------+---------+
AR.  -2.325   0.387  3.099                   (*-)
                            ---------+---------+---------+---------+
                                   -16         0        16        32
```

One-way ANOVA: Preliminary Samples Hardness Data

```
       Source   DF      SS     MS      F      P
       Factor    9  348.07  38.67  14.78  0.000
       Error   140  366.36   2.62
       Total   149  714.43
       S = 1.618   R-Sq = 48.72%   R-Sq(adj) = 45.42%
Individual 95% CIs For Mean Based on Pooled StDev
Level         N    Mean  StDev  ------+---------+---------+---------+---
15 s         15  72.713  2.277       (----*---)
15s          15  74.347  1.707                (---*---)
25s.         15  74.227  1.208               (---*---)
25 s         15  74.827  1.400                  (---*---)
35s          15  76.520  1.294                          (----*---)
35 s         15  75.673  0.878                      (---*---)
55 s         15  71.600  2.584  (---*---)
55s          15  71.660  2.026  (---*---)
As Received  15  74.153  0.414               (---*---)
As-received  15  74.540  1.119                 (---*---)
                            ------+---------+---------+---------+---
                               72.0      74.0      76.0      78.0
Pooled StDev = 1.618
Tukey 95% Simultaneous Confidence Intervals
All Pairwise Comparisons
Individual confidence level = 99.84%

15 s subtracted from:
              Lower  Center  Upper  ---------+---------+---------+---------+
15s          -0.267   1.633  3.534                   (-----*----)
25s.         -0.387   1.513  3.414                   (----*-----)
25 s          0.213   2.113  4.014                     (----*----)
35s           1.906   3.807  5.707                         (-----*----)
35 s          1.060   2.960  4.860                       (----*-----)
55 s         -3.014  -1.113  0.787            (-----*----)
55s          -2.954  -1.053  0.847             (----*----)
As Received  -0.460   1.440  3.340                   (----*-----)
As-received  -0.074   1.827  3.727                    (----*-----)
                            ---------+---------+---------+---------+
```

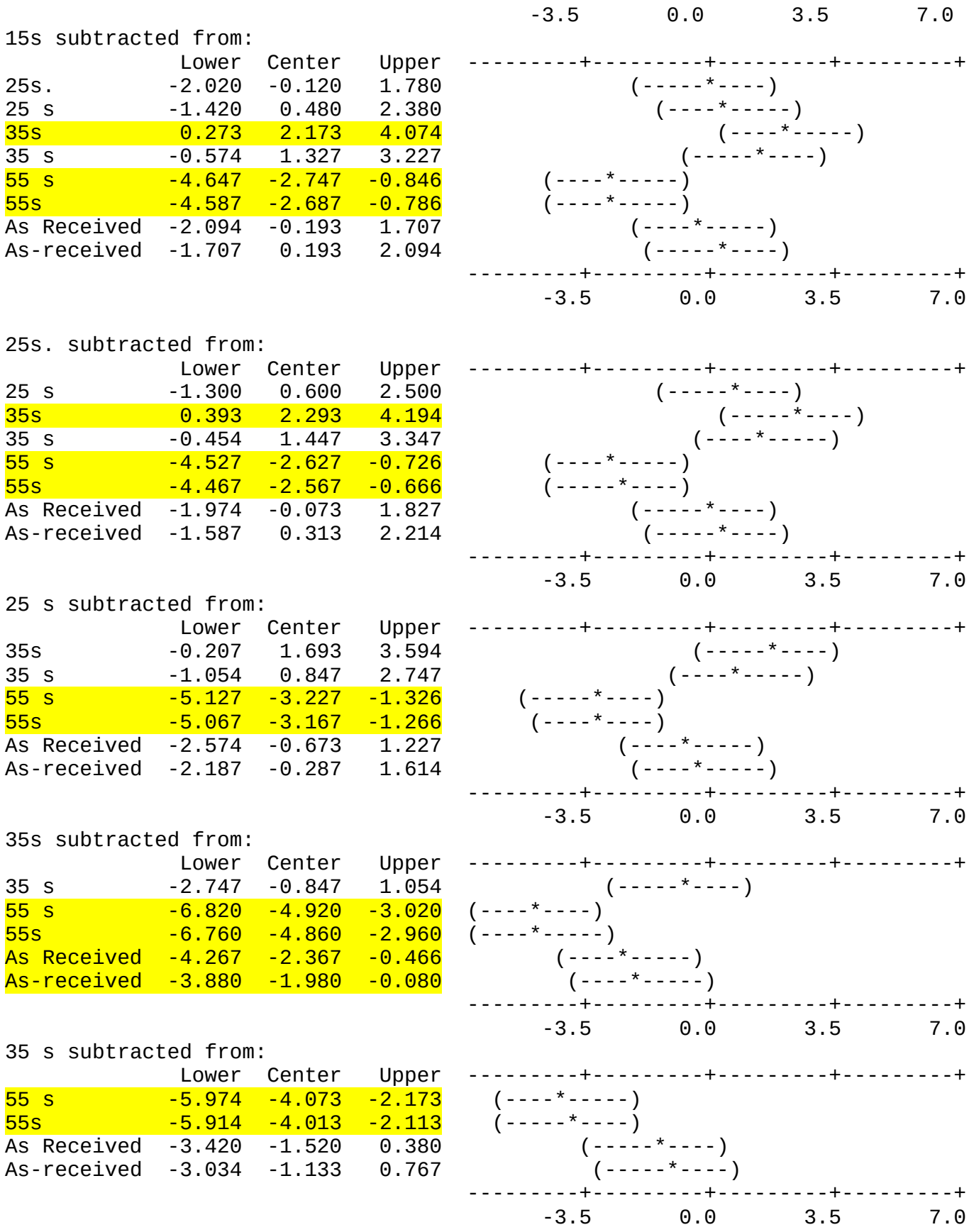
-3.5 0.0 3.5 7.0
15s subtracted from:
Lower Center Upper
25s. -2.020 -0.120 1.780
25 s -1.420 0.480 2.380
35s 0.273 2.173 4.074
35 s -0.574 1.327 3.227
55 s -4.647 -2.747 -0.846
55s -4.587 -2.687 -0.786
As Received -2.094 -0.193 1.707
As-received -1.707 0.193 2.094
-3.5 0.0 3.5 7.0
25s. subtracted from:
Lower Center Upper
25 s -1.300 0.600 2.500
35s 0.393 2.293 4.194
35 s -0.454 1.447 3.347
55 s -4.527 -2.627 -0.726
55s -4.467 -2.567 -0.666
As Received -1.974 -0.073 1.827
As-received -1.587 0.313 2.214
-3.5 0.0 3.5 7.0
25 s subtracted from:
Lower Center Upper
35s -0.207 1.693 3.594
35 s -1.054 0.847 2.747
55 s -5.127 -3.227 -1.326
55s -5.067 -3.167 -1.266
As Received -2.574 -0.673 1.227
As-received -2.187 -0.287 1.614
-3.5 0.0 3.5 7.0
35s subtracted from:
Lower Center Upper
35 s -2.747 -0.847 1.054
55 s -6.820 -4.920 -3.020
55s -6.760 -4.860 -2.960
As Received -4.267 -2.367 -0.466
As-received -3.880 -1.980 -0.080
-3.5 0.0 3.5 7.0
35 s subtracted from:
Lower Center Upper
55 s -5.974 -4.073 -2.173
55s -5.914 -4.013 -2.113
As Received -3.420 -1.520 0.380
As-received -3.034 -1.133 0.767
-3.5 0.0 3.5 7.0

```
55 s subtracted from:
              Lower  Center  Upper  ---------+---------+---------+---------+
55s          -1.840   0.060  1.960               (----*-----)
As Received   0.653   2.553  4.454                     (----*-----)
As-received   1.040   2.940  4.840                      (----*-----)
                                    ---------+---------+---------+---------+
                                          -3.5       0.0       3.5       7.0
55s subtracted from:
              Lower  Center  Upper  ---------+---------+---------+---------+
As Received   0.593   2.493  4.394                    (----*-----)
As-received   0.980   2.880  4.780                     (----*-----)
                                    ---------+---------+---------+---------+
                                         -3.5       0.0       3.5       7.0
As Received subtracted from:
              Lower  Center  Upper  ---------+---------+---------+---------+
As-received  -1.514   0.387  2.287               (----*-----)
                                    ---------+---------+---------+---------+
                                          -3.5       0.0       3.5       7.0
```

One-way ANOVA: Preliminary Samples Hardness Data

```
       Source   DF      SS     MS      F      P
       Factor    7  343.10  49.01  15.85  0.000
       Error   112  346.44   3.09
       Total   119  689.54
       S = 1.759   R-Sq = 49.76%   R-Sq(adj) = 46.62%
Individual 95% CIs For Mean Based on Pooled StDev
Level   N    Mean  StDev  ------+---------+---------+---------+--
15 s   15  72.713  2.277       (----*---)
15s    15  74.347  1.707               (----*---)
25s.   15  74.227  1.208               (---*----)
25 s   15  74.827  1.400                  (---*----)
35s    15  76.520  1.294                       (----*---)
35 s   15  75.673  0.878                     (---*----)
55 s   15  71.600  2.584  (---*---)
55s    15  71.660  2.026  (---*----)
                          ------+---------+---------+---------+--
                             72.0      74.0      76.0      78.0
Pooled StDev = 1.759
Tukey 95% Simultaneous Confidence Intervals
All Pairwise Comparisons
Individual confidence level = 99.75%

15 s subtracted from:
       Lower  Center  Upper    +---------+---------+---------+---------
15s   -0.351   1.633  3.618                      (-----*----)
25s.  -0.471   1.513  3.498                      (----*-----)
25 s   0.129   2.113  4.098                       (-----*-----)
35s    1.822   3.807  5.791                            (-----*-----)
35 s   0.976   2.960  4.944                         (----*-----)
55 s  -3.098  -1.113  0.871              (-----*----)
55s   -3.038  -1.053  0.931              (-----*-----)
```

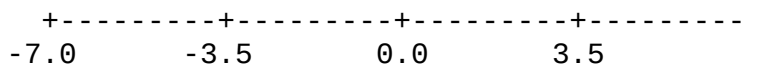

15s subtracted from:

	Lower	Center	Upper
25s.	-2.104	-0.120	1.864
25 s	-1.504	0.480	2.464
35s	0.189	2.173	4.158
35 s	-0.658	1.327	3.311
55 s	-4.731	-2.747	-0.762
55s	-4.671	-2.687	-0.702

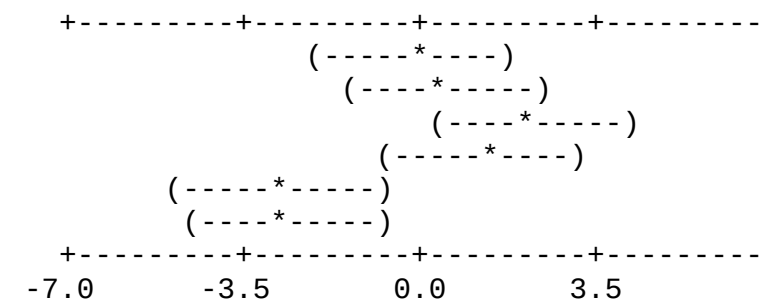

25s. subtracted from:

	Lower	Center	Upper
25 s	-1.384	0.600	2.584
35s	0.309	2.293	4.278
35 s	-0.538	1.447	3.431
55 s	-4.611	-2.627	-0.642
55s	-4.551	-2.567	-0.582

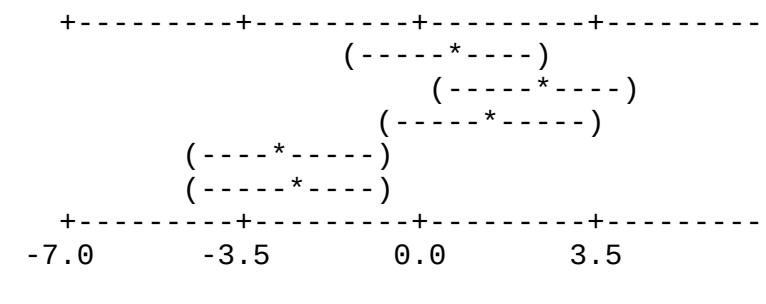

25 s subtracted from:

	Lower	Center	Upper
35s	-0.291	1.693	3.678
35 s	-1.138	0.847	2.831
55 s	-5.211	-3.227	-1.242
55s	-5.151	-3.167	-1.182

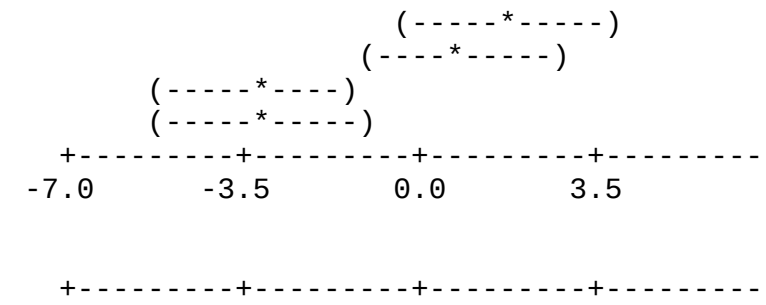

35s subtracted from:

	Lower	Center	Upper
35 s	-2.831	-0.847	1.138
55 s	-6.904	-4.920	-2.936
55s	-6.844	-4.860	-2.876

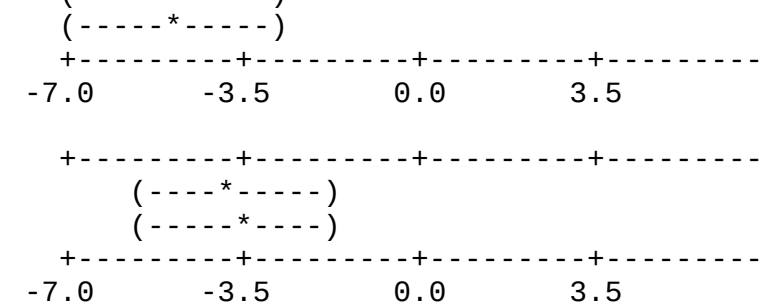

35 s subtracted from:

	Lower	Center	Upper
55 s	-6.058	-4.073	-2.089
55s	-5.998	-4.013	-2.029

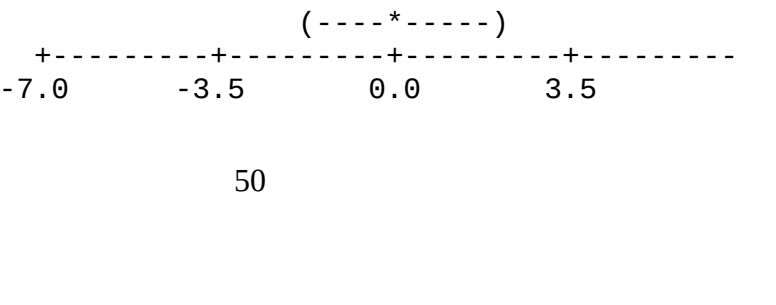

55 s subtracted from:

	Lower	Center	Upper
55s	-1.924	0.060	2.044

Appendix B: Tensile Stress Strain Curves for Quench Delays

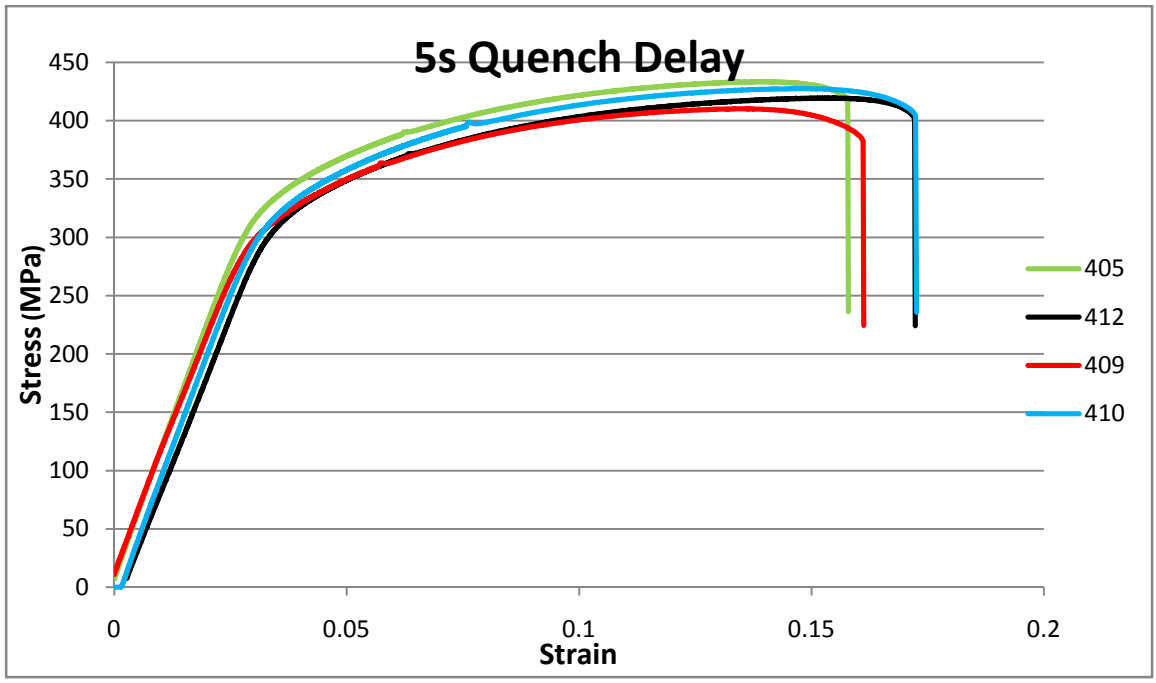

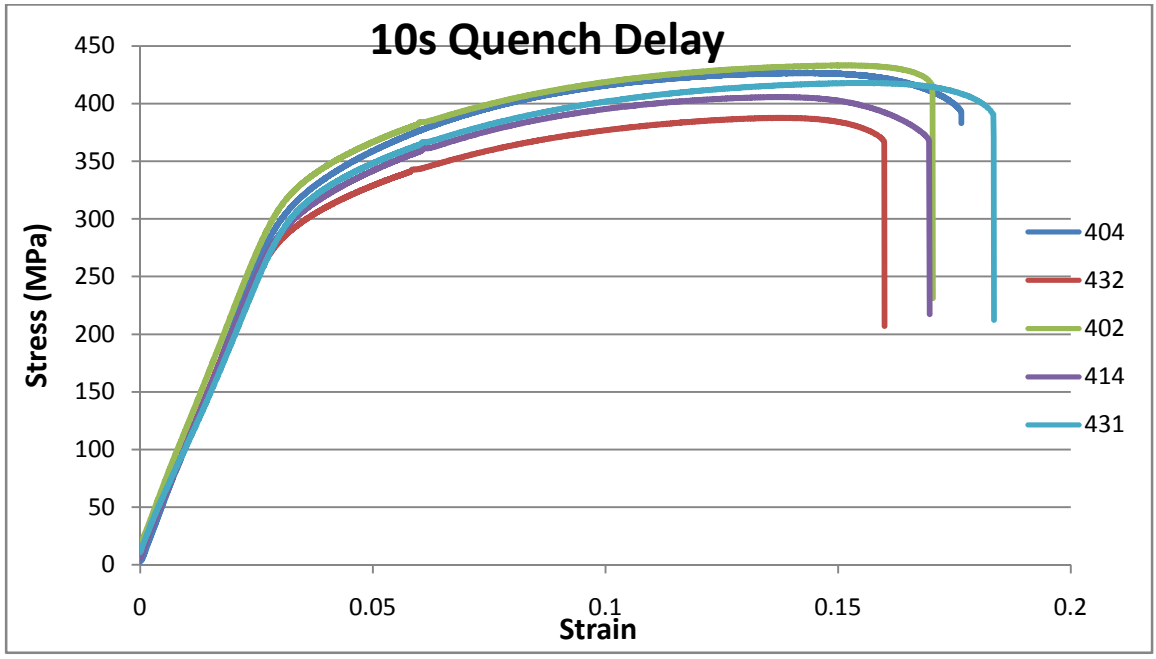

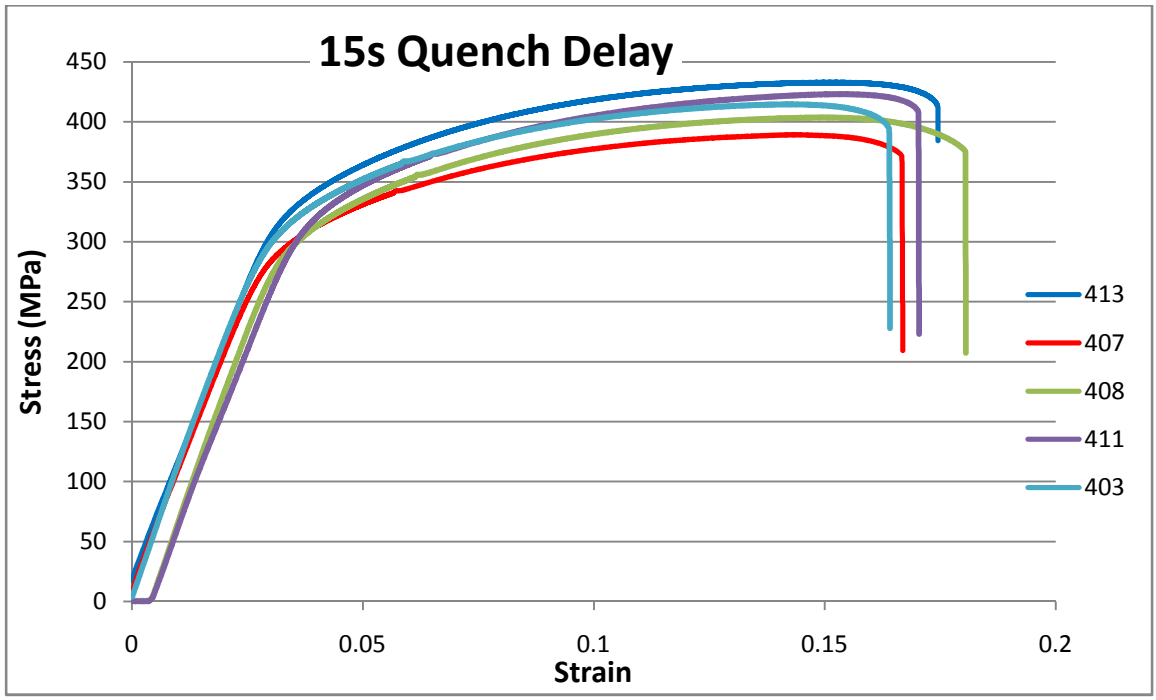
15s Quench Delay
Stress (MPa)
Strain
450
400
350
300
250
200
150
100
50
0
0
0.05
0.1
0.15
0.2
413
407
408
411
403

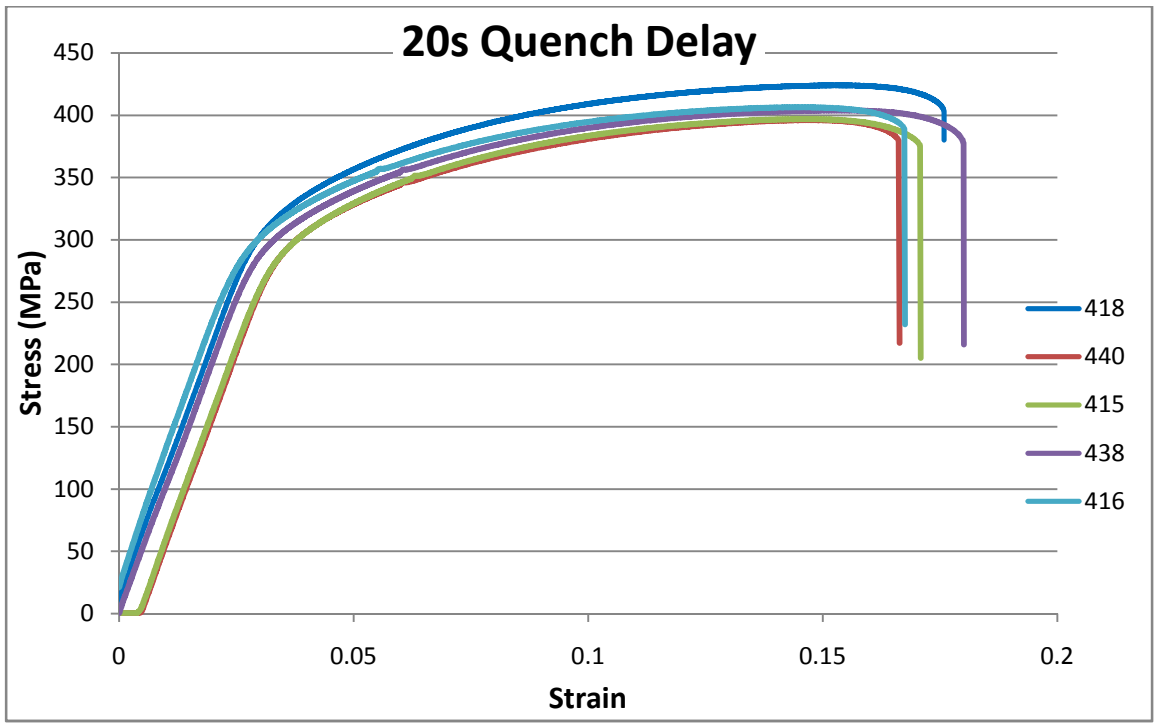
20s Quench Delay
Stress (MPa)
Strain
450
400
350
300
250
200
150
100
50
0
0
0.05
0.1
0.15
0.2
418
440
415
438
416

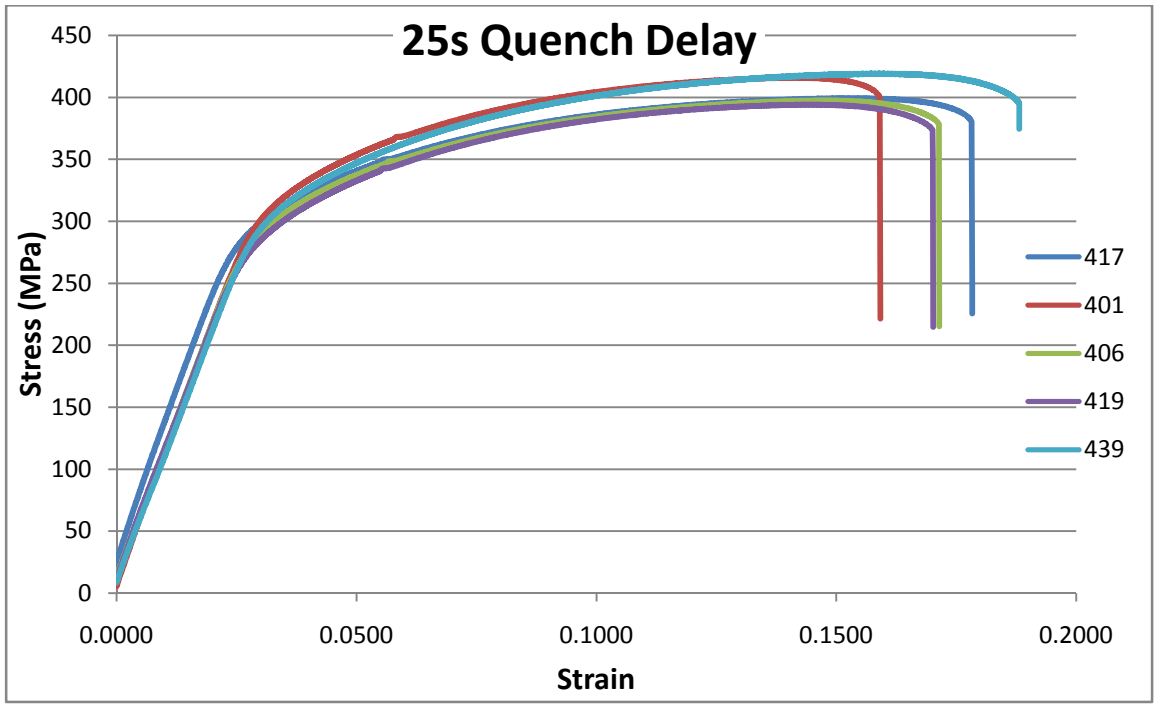
25s Quench Delay
Stress (MPa)
450
400
350
300
250
200
150
100
50
0
0.0000
0.0500
0.1000
0.1500
0.2000
Strain
417
401
406
419
439

Appendix C: Statistical Comparisons of Tensile Data

Tensile Strength

One-way ANOVA: Tensile Sample Tensile Strength

```
          Source  DF    SS   MS     F      P
          Factor   4  1292  323  1.63  0.205
          Error   20  3951  198
          Total   24  5243
          S = 14.06   R-Sq = 24.64%   R-Sq(adj) = 9.57%
Individual 95% CIs For Mean Based on Pooled StDev

Level   N    Mean  StDev  ---+---------+---------+---------+------
5s-TS   5  425.28  11.05                  (----------*----------)
10s-TS  5  414.18  18.25         (----------*----------)
15s-TS  5  412.54  17.16        (----------*----------)
20s-TS  5  405.58  11.39  (----------*----------)
25-TS   5  405.83  10.41  (----------*----------)
                          ---+---------+---------+---------+------
                           396       408       420       432
Pooled StDev = 14.06
Tukey 95% Simultaneous Confidence Intervals
All Pairwise Comparisons
Individual confidence level = 99.28%
5s-TS subtracted from:
         Lower  Center  Upper  ---------+---------+---------+---------+
10s-TS  -37.69  -11.10  15.49      (----------*---------)
15s-TS  -39.33  -12.74  13.85     (----------*----------)
20s-TS  -46.29  -19.70   6.89  (----------*----------)
25-TS   -46.04  -19.45   7.14   (----------*----------)
                              ---------+---------+---------+---------+
                                     -25         0        25        50
10s-TS subtracted from:
         Lower  Center  Upper  ---------+---------+---------+---------+
15s-TS  -28.23   -1.64  24.95         (---------*----------)
20s-TS  -35.19   -8.60  17.99       (----------*---------)
25-TS   -34.94   -8.35  18.24       (----------*---------)
                              ---------+---------+---------+---------+
                                     -25         0        25        50
15s-TS subtracted from:
         Lower  Center  Upper  ---------+---------+---------+---------+
20s-TS  -33.55   -6.96  19.63        (---------*----------)
25-TS   -33.30   -6.71  19.88        (---------*----------)
                              ---------+---------+---------+---------+
                                     -25         0        25        50
20s-TS subtracted from:
        Lower  Center  Upper  ---------+---------+---------+---------+
25-TS  -26.34    0.25  26.84         (----------*----------)
                            ---------+---------+---------+---------+
                                   -25         0        25        50
```

Yield Strength

One-way ANOVA: Tensile Sample Yield Strength

```
          Source  DF    SS   MS     F      P
          Factor   4  1300  325  2.85  0.061
          Error   15  1710  114
          Total   19  3010
          S = 10.68   R-Sq = 43.20%   R-Sq(adj) = 28.06%
Individual 95% CIs For Mean Based on Pooled StDev
Level   N    Mean  StDev  -----+---------+---------+---------+----
5s_YS   4  304.25   9.81                    (---------*--------)
10s_YS  4  294.50  15.02             (--------*---------)
15s_YS  4  291.00  10.95          (---------*--------)
20s_YS  4  284.50   4.04     (--------*---------)
25s_YS  4  281.25  10.56  (--------*---------)
                          -----+---------+---------+---------+----
                             276       288       300       312
Pooled StDev = 10.68
Tukey 95% Simultaneous Confidence Intervals
All Pairwise Comparisons

Individual confidence level = 99.25%
5s_YS subtracted from:
          Lower  Center  Upper  ---------+---------+---------+---------+
10s_YS  -33.08   -9.75  13.58        (--------*--------)
15s_YS  -36.58  -13.25  10.08     (---------*--------)
20s_YS  -43.08  -19.75   3.58   (--------*--------)
25s_YS  -46.33  -23.00   0.33  (---------*--------)
                              ---------+---------+---------+---------+
                                     -25         0        25        50
10s_YS subtracted from:
          Lower  Center  Upper  ---------+---------+---------+---------+
15s_YS  -26.83   -3.50  19.83          (---------*--------)
20s_YS  -33.33  -10.00  13.33        (--------*--------)
25s_YS  -36.58  -13.25  10.08     (---------*--------)
                              ---------+---------+---------+---------+
                                     -25         0        25        50
15s_YS subtracted from:
          Lower  Center  Upper  ---------+---------+---------+---------+
20s_YS  -29.83   -6.50  16.83         (--------*---------)
25s_YS  -33.08   -9.75  13.58       (--------*--------)
                              ---------+---------+---------+---------+
                                     -25         0        25        50
20s_YS subtracted from:
          Lower  Center  Upper  ---------+---------+---------+---------+
25s_YS  -26.58   -3.25  20.08          (---------*--------)
                              ---------+---------+---------+---------+
                                     -25         0        25        50
```